Journal of Computational and Applied Mathematics 234 (2010) 317–342

Contents lists available at ScienceDirect

Journal of Computational and Applied Mathematics

journal homepage: www.elsevier.com/locate/cam

A numerical comparison of Chebyshev methods for solving fourth order semilinear initial boundary value problems

B.K. Muite *

Mathematical Institute, University of Oxford, 24-29 St. Giles', Oxford OX1 3LB, UK

ARTICLE INFO

Article history:
Received 3 September 2008
Received in revised form 8 December 2009

Keywords:
Spectral collocation
Fast methods
Time stepping

ABSTRACT

In solving semilinear initial boundary value problems with prescribed non-periodic boundary conditions using implicit–explicit and implicit time stepping schemes, both the function and derivatives of the function may need to be computed accurately at each time step. To determine the best Chebyshev collocation method to do this, the accuracy of the real space Chebyshev differentiation, spectral space preconditioned Chebyshev tau, real space Chebyshev integration and spectral space Chebyshev integration methods are compared in the L^2 and $W^{2,2}$ norms when solving linear fourth order boundary value problems; and in the $L^\infty([0,T];L^2)$ and $L^\infty([0,T];W^{2,2})$ norms when solving initial boundary value problems. We find that the best Chebyshev method to use for high resolution computations of solutions to initial boundary value problems is the spectral space Chebyshev integration method which uses sparse matrix operations and has a computational cost comparable to Fourier spectral discretization.

Contents

* Tel.: +44 01865 273525; fax: +44 01865 273583.
E-mail address: muite@maths.ox.ac.uk.

0377-0427/$ – see front matter © 2009 Elsevier B.V. All rights reserved.
doi:10.1016/j.cam.2009.12.029

1. Introduction

The motivation for the comparison of these spectral methods is to compute solutions to high order semilinear initial boundary value problems found in elastodynamic models for microstructure formation during phase transitions in which a small Ginsburg or capillarity term is added. Typical examples of these semilinear initial boundary value problems can be found in studies in [1–3]. Many previous studies of microstructure formation with non-periodic boundary conditions have used low order finite difference or finite element methods, see, for example, Ahluwalia et al. [1], Vainchtein [4], Dondl and Zimmer [5] and the review in [6]. An objective of this study is to show that Chebyshev collocation methods efficiently simulate multiscale phenomena in regular but non-periodic domains and should be considered as a viable alternative to low order methods.

In a typical implicit–explicit (IMEX) or fully implicit time stepping scheme for an initial boundary value problem, not only is the function required at each time step, but derivatives of the function may also be required to calculate the explicit part of the time step or to perform fixed point or Newton iterations in a fully implicit time stepping scheme. To determine the best method to do this, the accuracy of approximate solutions and derivatives of approximate solutions obtained using different Chebyshev collocation methods in solving linear and initial boundary value problems are compared. The accuracy of solutions to linear boundary value problems are studied because in typical time stepping schemes, a linear boundary value problem is solved at each time step or iteration.

Chebyshev collocation methods have also been used to obtain high resolution numerical solutions to the KdV, Allen–Cahn and Cahn–Hilliard equations — see, for example, Xu and Tang [7] and Kassam and Trefethen [8]. They may also be useful in examining solutions to conservation laws, such as Burgers equation regularized by viscosity and dispersion, see, for example, Chen et al. [9] or Hesthaven et al. [10]. Here, numerical simulations can indicate the existence of possible vanishing viscosity or vanishing dispersion limits in bounded domains. Kaneda and Ishihara [11] have also used spectral methods to examine scaling laws for turbulent flow with periodic boundary conditions. As explained in [12] and in [13], it is also of interest to examine wall bounded flows. This can be done using Chebyshev spectral methods, for example Torres and Coutsias [14] use a mixed Chebyshev–Fourier discretization to solve the Navier–Stokes equations in a disk.

Following this introduction is a review of previous studies of Chebyshev collocation methods. The next sections contain a description and a comparison of the accuracy of the Chebyshev spectral integral, preconditioned Chebyshev differentiation and real space Chebyshev differentiation methods in solving linear boundary value problems. An IMEX and a fully implicit time stepping scheme that can use these Chebyshev spatial discretizations for solving initial boundary value problems are then described. Following this, the results of a numerical examination of the spatial and temporal convergence of the IMEX time stepping scheme for a model problem from the dynamics of phase transformations are summarized. In the final section we show that the fully implicit scheme can be used to simulate problems with stiff nonlinearities for which the IMEX scheme does not converge.

2. Previous work

There have been many studies of preconditioned Chebyshev and Chebyshev integration methods for boundary value problems, but none of these studies has numerically examined the accuracy of these methods in norms that include derivatives. The preconditioned Chebyshev tau method (hereafter referred to as the preconditioned Chebyshev differentiation to contrast it to the Chebyshev integration method) is described in [15, p. 119] and in [16, p. 173], and has been extended to general orthogonal polynomial expansions in [17]. Funaro and Heinrichs [18] and Tuckerman [19] have also discussed similar preconditioning methods for other orthogonal polynomial systems. Both the Chebyshev integration and preconditioned Chebyshev differentiation methods allow for the solution of linear boundary value problems in Chebyshev spectral space in $O(N)$ operations, and thus by using a Fast Fourier Transform, in $O(N \log N)$ operations in real space. Unfortunately, the preconditioned Chebyshev differentiation method does not immediately give derivatives of the function, and these must be obtained by differentiation. As has been noted in many studies, numerical differentiation of Chebyshev interpolants is sensitive to errors introduced by finite precision arithmetic in both real space (see, for example, Trefethen and Trummer [20] or Weideman and Trefethen [21]) and in spectral space if the spectral coefficients are not carefully computed (see, for example, Coutsias et al. [17] or Hesthaven et al. [10, p. 217]). Clenshaw [22] was the first documented user of the Chebyshev integration method in spectral space and El-Gendi [23,24] the first documented user of the Chebyshev integration method in real space. Greengard [25] showed that by using the Chebyshev spectral integration method to obtain numerical solutions to two-point linear boundary value problems in Chebyshev spectral space, it is possible to calculate derivatives without the numerical instability associated with differentiation. Coutsias et al. [17] generalized Greengard's results to expansions in other orthogonal polynomials and suggested methods to solve the resulting linear systems efficiently. It should be noted that Coutsias et al. [17] refer to the spectral space Chebyshev integration method as the postconditioned Chebyshev method to contrast it to the preconditioned Chebyshev method. However, the term integration better captures the notion that a smoothing operation which does not amplify errors occurs, and so this will be used here. Hiegemann [26] has also found that the spectral space Chebyshev integration method is useful for solving fourth order boundary value problems and that the small condition numbers of the resulting linear systems, makes it possible to solve them rapidly using iterative methods. Hiegemann [26] also demonstrates how to formulate the Chebyshev integration method for non-constant coefficient linear boundary value problems and for time dependent problems. A recent implementation of the real space Chebyshev integration method can be found in [27].

The Chebyshev integration method in spectral space has so far primarily been used in IMEX schemes for initial boundary value problems with at most two spatial derivatives, for example in [14,28,29]. Clenshaw [22] and Elliot [30] have also used versions of the Chebyshev integration method in spectral space for linear two-point boundary value problems and for the time-dependent heat equation respectively; however, because their papers were published in 1957 and 1960, the advantages of their method in comparison to other numerical methods in use today are not indicated. Khater and Temsah [31,32] have used the real space Chebyshev integration method to solve third, fourth and fifth order semilinear initial boundary value problems.

Zebib [33] has also shown that, by solving for the highest derivative in a fourth order nonlinear boundary value problem and then integrating to obtain the lower order derivatives, the accuracy of Galerkin solutions to nonlinear boundary value problems can be improved. When using a full Galerkin method, an iterative solution of the resulting nonlinear equations is required. Zebib [33] found that it was computationally expensive to use Newton iteration scheme with a large number of modes when high spatial resolution simulations were required.

Mai-Duy [34] and Mai-Duy and Tanner [35] have also compared the accuracy in the L^2 norm of the real space Chebyshev collocation differentiation and spectral space Chebyshev collocation integration methods to obtain solutions to linear fourth order boundary value problems. They found that the Chebyshev integration method in spectral space gave more accurate results than the Chebyshev collocation differentiation method. They did not use a large number of modes, nor did they examine the accuracy of the method in norms which included derivatives, so they did not show when the extra effort of using the integration method instead of the collocation differentiation method is justified.

Most implementations of the Chebyshev integration method have been in Chebyshev spectral where the sparse matrix structure leads to a low operation count and hence allows for fast algorithms when many discretization points are used. It is also possible to formulate the Chebyshev integration method in real space which avoids the use of the Fast Fourier Transform, but requires the use of dense matrices. A recent implementation of this method can be found in [36]. Driscoll [37], Deloff [38], Mihalia and Mihalia [39] and Stern [40] have found that the Chebyshev integration method in real space is useful for solving the Schrödinger equation — a particularly interesting observation is that the method can be used to solve boundary value problems which have continuous solutions, but have discontinuous derivatives.

3. Boundary value problems

In this section, the real space Chebyshev differentiation, the spectral space preconditioned Chebyshev differentiation, the Chebyshev integration method in spectral space and the Chebyshev integration method in real space are described. It is implicitly assumed that space is discretized using a collocation scheme with Chebyshev polynomials of the first kind so that

$$T_n(x) := \cos n \cos^{-1} x,$$

with x evaluated at the Chebyshev Gauss–Lobatto points,

$$x_i := \cos \frac{\pi i}{N}, \quad i = 0, \ldots, N.$$

The reason for using this discretization is that it allows the use of the Fast Fourier Transform to calculate integrals and derivatives when computing solutions.

3.1. Spatial discretization

We explain the differences between the different Chebyshev methods by considering the linear boundary value problem

$$\begin{aligned} &Aw_{xxxx} + Bw_{xx} + Cw = f(x) \\ &w(-1) = 0, \qquad w(1) = 0, \qquad w_x(-1) = 0, \qquad w_x(1) = 0, \end{aligned} \tag{3.1}$$

where w is the displacement, A, B and C are constants, $x \in [-1, 1]$ is the position and $f(x)$ is a smooth but otherwise unrestricted function.

3.1.1. The real space Chebyshev differentiation method

The Chebyshev differentiation matrix method as described in [41, p. 145] amounts to solving the following linear matrix equation

$$\left(A\bar{\boldsymbol{D}}^4 + B\boldsymbol{D}^2 + C\boldsymbol{I}\right)\boldsymbol{w} = \boldsymbol{f}. \tag{3.2}$$

Here $\boldsymbol{D}^k$ is the real space Chebyshev differentiation matrix of order k, $\bar{\boldsymbol{D}}^4$ is a modification of the fourth order real space Chebyshev differentiation matrix which has been changed to ensure that the approximate solution satisfies the boundary conditions given in Eq. (3.2), $\boldsymbol{I}$ is the identity matrix, $\boldsymbol{w}$ is a vector with the approximate solution values for w at the nodal points, and $\boldsymbol{f}$ is a vector with the forcing function values at the nodal points. As explained in [41, p. 58] and in [16, p. 88], the formulas for the entries in the matrix $\boldsymbol{D}$ can be derived by differentiating interpolating polynomials and evaluating the derivatives at the nodal points. The entries for $\boldsymbol{D}$ are given by the following theorem, the statement of which is taken from Trefethen [41, p. 53].

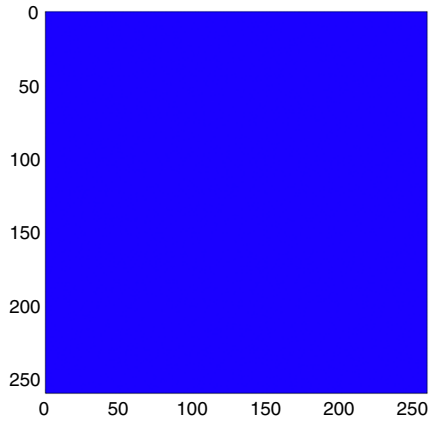

Fig. 1. Sparsity pattern of the discretized real space boundary value problem differentiation operator $\bar{\boldsymbol{D}}^4 + \boldsymbol{D}^2 + \boldsymbol{I}$ with 257 Chebyshev modes. The figure shows that the matrix is dense and should be compared with Figs. 2–4 for the other implementations of Chebyshev collocation methods.

Theorem 3.1 (*Chebyshev Differentiation Matrix*). *For each $N \geq 1$, let the rows and columns of the $(N+1) \times (N+1)$ Chebyshev spectral differentiation matrix $\boldsymbol{D}$ be indexed from 0 to N. The entries of this matrix are*

$$(\boldsymbol{D})_{00} = \frac{2N^2+1}{6}, \qquad (D_N)_{NN} = -\frac{2N^2+1}{6} \tag{3.3}$$

$$(\boldsymbol{D})_{jj} = \frac{-x_j}{2(1-x_j^2)}, \quad j = 1, \ldots, N-1 \tag{3.4}$$

$$(\boldsymbol{D})_{ij} = \frac{c_i}{c_j}\frac{(-1)^{(1+j)}}{(x_i - x_j)}, \quad i \neq j,\ i, j = 0, \ldots, N \tag{3.5}$$

where

$$c_i := \begin{cases} 2, & i = 0 \text{ or } N, \\ 1, & \text{otherwise.} \end{cases}$$

In all computational experiments considered here, $\boldsymbol{D}$ was obtained using the function `cheb.m` which can be found in [41, p. 58]. This function does not use the formulas in Theorem 3.1 directly, but uses a more numerically stable implementation, a further discussion of numerically stable implementations for Chebyshev differentiation matrices can be found in [10, p. 217].

Note that the solution of the linear system in Eq. (3.2), only gives $\boldsymbol{w}$ and not its derivatives. Note also that $\bar{\boldsymbol{D}}^4 \neq (\boldsymbol{D}^1)^4$ because the highest order differentiation matrix is modified to ensure that the solution satisfies clamped boundary conditions. To be precise, as explained in [41, p. 146], we restrict our search for polynomial interpolants that satisfy the boundary conditions by obtaining solutions in polynomials that have $(1 - x^2)$ as a factor. Thus, if $x_i \in [0, 1]$ is the ith Chebyshev Gauss–Lobatto node and $\boldsymbol{x}$ is a vector with the node locations, then

$$\bar{\boldsymbol{D}}^4 = \left[\text{diag}(1-\boldsymbol{x}^2)\boldsymbol{D}^4 - 8\text{diag}(\boldsymbol{x})\boldsymbol{D}^3 - 12\boldsymbol{D}^2\right] \times \text{diag}\left[\frac{1}{1-\boldsymbol{x}^2}\right]$$

where $\text{diag}(\boldsymbol{x})$ is a diagonal matrix whose entries are from the vector $\boldsymbol{x}$. As shown in Fig. 1, the resulting differentiation matrices are full, so solving the large linear systems using these matrices can take some time when many discretization points are used.

3.1.2. The spectral space preconditioned Chebyshev differentiation method

The fourth order real space Chebyshev differentiation matrices have a condition number of $O(N^8)$ and are dense. As explained in [21], it is therefore difficult to use this method when a large number of grid points are required. A more suitable method is the preconditioned differentiation method which has a condition number of $O(N^4)$ and is sparse. To obtain the preconditioned differentiation method as described in [15, p. 119], Eq. (3.2) is transformed into an equation for the coefficients of the truncated Chebyshev expansions for w and f, denoted by $\hat{\boldsymbol{w}}$ and $\hat{\boldsymbol{f}}$ respectively. The resulting infinite system of equations is truncated, to obtain

$$\left(A\hat{\boldsymbol{D}}^4 + B\hat{\boldsymbol{D}}^2 + C\boldsymbol{I}\right)\hat{\boldsymbol{w}} = \hat{\boldsymbol{f}}, \tag{3.6}$$

where $\hat{\boldsymbol{D}}^k$ is the kth order Chebyshev differentiation matrix in Chebyshev spectral space (the entries of these spectral differentiation matrices can be found in [10, p. 258] or in [17]). The resulting equations are then multiplied by the highest

order integration matrix to obtain the sparse system of equations

$$\left(A\widehat{\boldsymbol{PD}}^4 + B\widehat{\boldsymbol{PD}}^2 + C\widehat{\boldsymbol{PD}}^0 + \hat{\boldsymbol{LBC1}}\right)\hat{\boldsymbol{w}} = \widehat{\boldsymbol{PD}}^4\hat{\boldsymbol{f}} + \widehat{\boldsymbol{RBC1}}. \tag{3.7}$$

Here $\widehat{\boldsymbol{PD}}^k$ is the preconditioned Chebyshev differentiation matrix of order k in which the four rows for the coefficients of the four highest order Chebyshev polynomials have been set to zero, $\hat{\boldsymbol{w}}$ is the vector with coefficients for each Chebyshev polynomial for the approximation of w and $\hat{\boldsymbol{f}}$ is the vector with the coefficients for each Chebyshev polynomial for the approximation of f. The reason for setting the first four rows in the matrices $\widehat{\boldsymbol{PD}}^k$ to zero is that the equations for the highest modes are used to enforce the boundary conditions exactly, instead of satisfying the differential equation. Thus $\hat{\boldsymbol{LBC1}}$ contains the coefficients for the boundary conditions in Chebyshev spectral space and $\widehat{\boldsymbol{RBC1}}$ contains the values of these boundary conditions.

We now describe how to find the entries of the fourth order preconditioned Chebyshev differentiation matrices. We do so by extending Gottlieb and Orszag's [15, p. 119] second order preconditioned Chebyshev differentiation matrix approach. The formulas for the fourth order preconditioned Chebyshev differentiation matrices are similar to those for the second order preconditioned Chebyshev differentiation matrices, but, as they are not available elsewhere, we give them here. The presentation is similar to that in [16, p. 173] and [15, p. 119] for second order linear boundary value problems.

We expand g, w, w_{xx} and w_{xxxx} in Eq. (3.1), in terms of Chebyshev polynomials,

$$g = \sum_{n=0}^{\infty} g_n T_n(x), \qquad w = \sum_{n=0}^{\infty} a_n T_n(x), \qquad w_{xx} = \sum_{n=0}^{\infty} a_n'' T_n(x)$$

$$\text{and} \quad w_{xxxx} = \sum_{n=0}^{\infty} a_n'''' T_n(x).$$

We equate modal coefficients in Eq. (3.1),

$$Aa_n + Ba_n'' + Ca_n'''' = g_n. \tag{3.8}$$

We now consider approximations of w, w_{xx} and w_{xxxx} obtained by finite Chebyshev series with $N+1$ terms. The preconditioned matrices can be found from a relationship between a_n, a_n'', and a_n'''' by using the recursion relation

$$2na_n = c_{n-1}a_{n-1}' - a_{n+1}', \tag{3.9}$$

where

$$c_n := \begin{cases} 0, & n < 0 \quad \text{or} \quad n > N, \\ 2, & n = 0, \\ 1, & \text{otherwise.} \end{cases}$$

This recursion relation can be found in [16, p. 87] or [15, p. 161]. Using Eq. (3.9) repeatedly we find that

$$a_n = c_{n-1}\frac{a_{n-1}'}{2n} - \frac{a_{n+1}'}{2n}, \tag{3.10}$$

$$a_n = \frac{c_{n-1}c_{n-2}}{4n(n-1)}a_{n-2}'' - \left[\frac{c_{n-1}}{4n(n-1)} + \frac{c_n}{4n(n+1)}\right]a_n'' + \frac{1}{4n(n+1)}a_{n+2}'', \tag{3.11}$$

$$\begin{aligned} a_n \;=\; & \frac{c_{n-1}c_{n-2}c_{n-3}}{8n(n-1)(n-2)}a_{n_3}''' - \left[\frac{c_{n-1}c_{n-2}}{8n(n-1)(n-2)} + \frac{c_{n-1}^2}{8n^2(n-1)} + \frac{c_nc_{n-1}}{8(n+1)n^2}\right]a_{n-1}''' \\ & + \left[\frac{c_{n-1}}{8n^2(n-1)} + \frac{c_n}{8(n+1)n^2} + \frac{c_{n+1}}{8(n+2)(n+1)n}\right]a_{n+1}''' - \frac{1}{8(n+2)(n+1)n}a_{n+3}''', \end{aligned} \tag{3.12}$$

$$\begin{aligned} a_n \;=\; & \frac{c_{n-1}c_{n-2}c_{n-3}c_{n-4}}{16n(n-1)(n-2)(n-3)}a_{n-4}'''' - \left[\frac{c_{n-1}c_{n-2}c_{n-3}}{16n(n-1)(n-2)(n-3)} + \frac{c_{n-1}c_{n-2}^2}{16n(n-1)^2(n-2)}\right. \\ & \left. + \frac{c_{n-1}^2c_{n-2}}{16n^2(n-1)^2} + \frac{c_nc_{n-1}c_{n-2}}{16(n+1)n^2(n-1)}\right]a_{n-2}'''' + \left[\frac{c_{n-1}c_n}{16n(n-1)^2(n-2)} + \frac{c_{n-1}^2}{16n^2(n-1)^2}\right. \\ & \left. + \frac{c_nc_{n-1}}{16(n+1)n^2(n-1)} + \frac{c_nc_{n-1}}{16(n+1)n^2(n-1)} + \frac{c_n^2}{16(n+1)^2n^2} + \frac{c_{n+1}c_n}{16(n+1)^2n^2}\right]a_n'''' \\ & - \left[\frac{c_{n-1}}{16(n+1)n^2(n-1)} + \frac{c_n}{16(n+1)^2n^2} + \frac{c_{n+1}}{16(n+2)(n+1)^2n} + \frac{c_{n+2}}{16(n+3)(n+2)(n+1)n}\right]a_{n+2}'''' \\ & + \frac{1}{16(n+3)(n+2)(n+1)n}a_{n+4}''''. \end{aligned} \tag{3.13}$$

Eqs. (3.10)–(3.13) are now used to obtain a sparse matrix system for Eq. (3.1). Eq. (3.13) is of the form,

$$a_n = \mu_1 a''''_{n-4} + \mu_2 a''''_{n-2} + \mu_3 a''''_n + \mu_4 a''''_{n+2} + \mu_5 a''''_{n+4}, \tag{3.14}$$

where after some simplification and using the fact that we are interested in coefficients for $4 \le n \le N$ to eliminate c_n, we find that

$$\mu_{1n} := \frac{c_{n-4}}{16n(n-1)(n-2)(n-3)}, \qquad \mu_{2n} := -\frac{1}{4(n+1)n(n-1)(n-3)},$$
$$\mu_{3n} := \frac{3}{8(n+2)(n+1)(n-1)(n-2)}, \qquad \mu_{4n} := -\frac{1}{4(n+3)(n+1)n(n-1)}$$

and

$$\mu_{5n} := \frac{1}{16(n+3)(n+2)(n+1)n}. \tag{3.15}$$

Eliminating a''''_n from Eq. (3.8) by using Eq. (3.13) gives,

$$\begin{aligned} &A\left(\mu_{1n}a_{n-4} + \mu_{2n}a_{n-2} + \mu_{3n}a_n + d_{n+2}\mu_{4n}a_{n+2} + d_{n+4}\mu_{5n}a_{n+4}\right) \\ &\quad + B\left(\mu_{1n}a''_{n-4} + \mu_{2n}a''_{n-2} + \mu_{3n}a''_n + d_{n+2}\mu_{4n}a''_{n+2} + d_{n+4}\mu_{5n}a''_{n+4}\right) + Ca_n \\ &\quad = \left(\mu_{1n}g_{n-4} + \mu_{2n}g_{n-2} + \mu_{3n}g_n + d_{n+2}\mu_{4n}g_{n+2} + d_{n+4}\mu_{5n}g_{n+4}\right), \end{aligned} \tag{3.16}$$

which holds for $4 \le n \le N$ and for which

$$d_n := \begin{cases} 0, & n < 0 \quad \text{or } n > N, \\ 1, & \text{otherwise.} \end{cases}$$

We now eliminate $a''_{n-4}, \ldots, a''_{n+4}$ from Eq. (3.16). To do so Eq. (3.11) is used along with the observation that

$$\mu_{1n}a''_{n-4} + \mu_{2n}a''_{n-2} + \mu_{3n}a''_n + \mu_{4n}a''_{n+2} + \mu_{5n}a''_{n+4} = \nu_{1n}a_{n-2} + \nu_{2n}a_n + \nu_{3n}a_{n+2}, \tag{3.17}$$

where after some simplification and again using the fact that we are interested in the case $4 \le n \le N$ to eliminate c_n, we find that

$$\nu_{1n} = \frac{1}{4n(n-1)}, \qquad \nu_{2n} = -\frac{1}{2(n-1)(n+1)} \quad \text{and} \quad \nu_{3n} = \frac{1}{4n(n+1)}. \tag{3.18}$$

The final matrix system is

$$\begin{aligned} &A\left(\mu_{1n}a_{n-4} + \mu_{2n}a_{n-2} + \mu_{3n}a_n + d_{n+2}\mu_{4n}a_{n+2} + d_{n+4}\mu_{5n}a_{n+4}\right) \\ &\quad + B\left(\nu_{1n}a_{n-2} + \nu_{2n}a_n + d_{n+2}\nu_{3n}a_{n+2}\right) + Ca_n \\ &\quad = \left(\mu_{1n}g_{n-4} + \mu_{2n}g_{n-2} + \mu_{3n}g_n + d_{n+2}\mu_n g_{n+2} + d_{n+4}\mu_{5n}g_{n+4}\right), \end{aligned} \tag{3.19}$$

which holds for $4 \le n \le N$. This gives a system of $N+1$ unknowns and $N+3$ equations. The last four equations are obtained from the boundary conditions, $w(\pm 1) = 0$ and $w_x(\pm 1) = 0$. We use the values of the Chebyshev polynomials and their first derivatives at $x = \pm 1$, which are

$$T_n(\pm 1) = (\pm 1)^n \quad \text{and} \quad \frac{\mathrm{d}T_n}{\mathrm{d}x}(\pm 1) = (\pm 1)^{n+1}n^2,$$

and can be found in [10, p. 258]. The equations for the boundary conditions are then

$$0 = \sum_{n=0}^{N} (\pm 1)^n a_n \quad \text{and} \quad 0 = \sum_{n=0}^{N} (\pm 1)^{n+1} n^2 a_n. \tag{3.20}$$

This set of equations corresponds to the matrix system

$$\left(A\hat{\boldsymbol{P}}\hat{\boldsymbol{D}}^0 + B\hat{\boldsymbol{P}}\hat{\boldsymbol{D}}^2 + C\hat{\boldsymbol{P}}\hat{\boldsymbol{D}}^4 + \boldsymbol{L}\hat{\boldsymbol{B}}\boldsymbol{C1}\right)\hat{\boldsymbol{w}} = \hat{\boldsymbol{P}}\hat{\boldsymbol{D}}^0\hat{\boldsymbol{g}} + \boldsymbol{R}\hat{\boldsymbol{B}}\boldsymbol{C1}, \tag{3.21}$$

in which $\hat{\boldsymbol{w}}$ is a vector with the coefficients for the Chebyshev series of w, the equations for the boundary conditions are in $\boldsymbol{L}\hat{\boldsymbol{B}}\boldsymbol{C1}$ and $\boldsymbol{R}\hat{\boldsymbol{B}}\boldsymbol{C1}$ contains the values of these boundary conditions.

Note again that, the linear system in Eq. (3.7) is solved to find an approximate solution to w, and thus this solution needs to be differentiated numerically to obtain approximations of the derivatives of the exact solution. This differentiation can either be done in spectral space by using the dense upper triangular spectral differentiation matrices shown in Fig. 2(b), which, if there are N modes, requires $O(N^2)$ operations, or by transforming to real space and using the Fast Fourier Transform to differentiate the resulting series, (see, for example, Trefethen [41, p. 78]) which requires $O(N \log N)$ operations. The sparsity pattern for the preconditioned matrix operator is shown in Fig. 2(a). Since this matrix is sparse, the solution of the system of equations in Eq. (3.7) requires $O(N)$ operations.

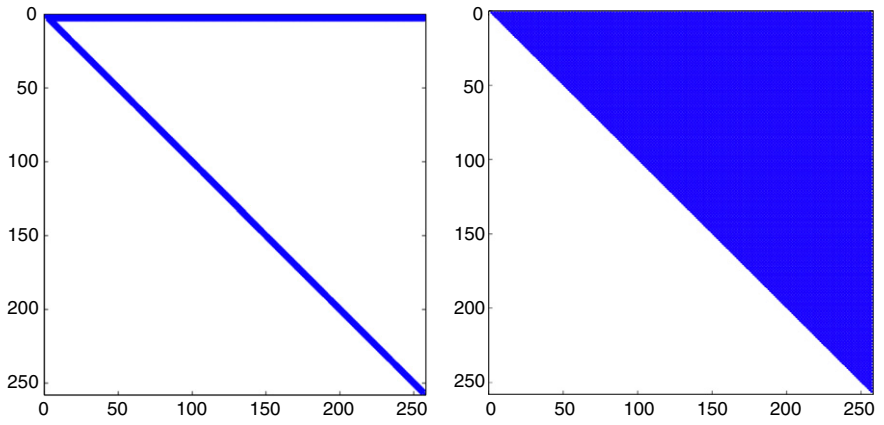

(a) Discretized spectral space Chebyshev preconditioned boundary value problem differentiation operator $\widehat{\boldsymbol{PD}}^0 + \widehat{\boldsymbol{PD}}^2 + \widehat{\boldsymbol{PD}}^4 + \widehat{\boldsymbol{LBC1}}$.

(b) Discretized spectral space Chebyshev differentiation operator $\boldsymbol{D}$.

Fig. 2. Sparsity patterns for the preconditioned Chebyshev space differentiation method with 257 Chebyshev modes, compare with Figs. 1, 3 and 4 for the other collocation Chebyshev methods studied here.

3.1.3. The spectral space Chebyshev integration method

Greengard [25] explains that the Chebyshev integration method amounts to solving for the highest order derivative once Eq. (3.2) is transformed into an equation for the truncated Chebyshev expansions of w and $f(x)$

$$\left(A\hat{\boldsymbol{S}}^0 + B\hat{\boldsymbol{S}}^2 + C\hat{\boldsymbol{S}}^4 + \widehat{\boldsymbol{LBC2}}\right)\hat{\boldsymbol{w}}_{xxxx} = \hat{\boldsymbol{f}} + \widehat{\boldsymbol{RBC2}}. \tag{3.22}$$

In this equation, $\widehat{\boldsymbol{LBC2}}$ is a matrix with the equations that the coefficients of the Chebyshev expansion should satisfy, $\widehat{\boldsymbol{RBC2}}$ is a vector with the values of these boundary conditions and $\hat{\boldsymbol{w}}_{xxxx}$ is a vector with the coefficients of the truncated series expansion for w_{xxxx}. The matrix $\widehat{\boldsymbol{LBC2}}$ and vector $\widehat{\boldsymbol{RBC2}}$ fix the four coefficients obtained from the indefinite integral of w_{xxxx} by using the boundary conditions. This linear system is solved to find $\hat{\boldsymbol{w}}_{xxxx}$, which is then integrated to find $\hat{\boldsymbol{w}}$ and its first three derivatives.

The implementations of Chebyshev integration matrices that have been used in the literature differ. An implementation for fourth order problems has been given in [27], but it is slightly different than the one we use here, and so we include all the details of the construction of these matrices. To obtain the Chebyshev integration matrices, we use the following indefinite integral identities (see, for example, Hesthaven et al. [10, p. 257]):

$$\int T_0(x) = T_1(x), \qquad \int T_1(x) = \frac{T_2(x)}{4} \quad \text{and} \quad \int T_n(x) = \frac{T_{n+1}(x)}{2(n+1)} - \frac{T_{n-1}(x)}{2(n-1)}.$$

Suppose

$$w_{xxxx} = \sum_{n=0}^{\infty} b_n T_n(x). \tag{3.23}$$

Then by using the indefinite integral identities we find that

$$w_{xxx} = e_3 + \left(b_0 - \frac{b_2}{2}\right) T_1(x) + \sum_{n=2}^{\infty} \left(\frac{b_{n-1} - b_{n+1}}{2n}\right) T_n(x), \tag{3.24}$$

$$\begin{aligned} w_{xx} \;=\; & e_2 + \left(e_3 - \frac{b_1}{8} + \frac{b_3}{8}\right) T_1(x) + \left(\frac{b_0}{4} - \frac{b_2}{6} + \frac{b_4}{24}\right) T_2(x) \\ & + \sum_{n=3}^{\infty} \left(\frac{b_{n-2}}{4n(n-1)} - \frac{b_n}{2(n-1)(n+1)} + \frac{b_{n+2}}{4n(n+1)}\right) T_n(x), \end{aligned} \tag{3.25}$$

$$\begin{aligned} w_x \;=\; & e_1 + \left(e_2 - \frac{b_0}{8} + \frac{b_2}{12} - \frac{b_4}{48}\right) T_1(x) + \left(\frac{e_3}{4} - \frac{b_1}{24} + \frac{3b_3}{64} - \frac{b_5}{192}\right) T_2(x) + \left(\frac{b_0}{24} - \frac{b_2}{32} + \frac{b_4}{80} - \frac{b_6}{480}\right) T_3(x) \\ & + \sum_{n=4}^{\infty} \left(\frac{b_{n-3}}{8n(n-1)(n-2)} - \frac{3b_{n-1}}{8(n+1)n(n-2)} + \frac{3b_{n+1}}{8(n+2)n(n-1)} - \frac{b_{n+3}}{8(n+2)(n+1)n}\right) T_n(x), \end{aligned} \tag{3.26}$$

and

$$w = e_0 + \left(e_1 - \frac{e_3}{8} + \frac{b_1}{48} - \frac{3b_3}{128} + \frac{b_5}{384}\right) T_1(x) + \left(\frac{e_2}{4} - \frac{b_0}{24} + \frac{11b_2}{384} - \frac{b_4}{120} + \frac{b_6}{1920}\right) T_2(x)$$
$$+ \left(\frac{e_3}{24} - \frac{b_1}{128} + \frac{3b_3}{320} - \frac{b_5}{576} + \frac{b_7}{5760}\right) T_3(x) + \left(\frac{b_0}{192} - \frac{b_2}{240} + \frac{b_4}{480} - \frac{b_6}{1680} + \frac{b_8}{13\,440}\right) T_4(x)$$
$$+ \sum_{n=5}^{\infty} \left(\frac{b_{n-4}}{16n(n-1)(n-2)(n-3)} - \frac{b_{n-2}}{4(n+1)n(n-1)(n-3)} + \frac{3b_n}{8(n+2)(n+1)(n-1)(n-2)} \right.$$
$$\left. - \frac{b_{n+2}}{4(n+3)(n+1)n(n-1)} + \frac{b_{n+4}}{16(n+3)(n+2)(n+1)n} \right) T_n(x). \tag{3.27}$$

In these equations, e_i are constants of integration and b_i are the coefficients of the Chebyshev series for w_{xxxx}. To implement the method numerically, this infinite system of equations must be truncated. If there are $N+1$ modes for w_{xxxx}, then the linear system above has $N+5$ coefficients, one for each Chebyshev mode and 4 coefficients to be satisfied by the boundary conditions.

After transforming the functions into the space of Chebyshev polynomials, the resulting equation for the integration matrices is

$$\left(A\hat{\boldsymbol{S}}^4 + B\hat{\boldsymbol{S}}^2 + C\hat{\boldsymbol{S}}^0 + \widehat{\boldsymbol{LBC2}}\right) \hat{\boldsymbol{w}}_{xxxx} = \hat{\boldsymbol{g}} + \widehat{\boldsymbol{RBC2}},$$

in which the spectral integration matrix of order k is denoted by $\hat{\boldsymbol{S}}^k$. This system of equations is used to define each spectral integration matrix. This system of equations is explicitly given by

$$Ae_0 + Be_2 + Cb_0 = g_0,$$
$$A\left(e_1 - \frac{e_3}{8} + \frac{b_1}{48} - \frac{3b_3}{128} + \frac{b_5}{384}\right) + B\left(e_3 - \frac{b_1}{8} + \frac{b_3}{8}\right) + Cb_1 = g_1,$$
$$A\left(\frac{e_2}{4} - \frac{b_0}{24} + \frac{11b_2}{384} - \frac{b_4}{120} + \frac{b_6}{1920}\right) + B\left(\frac{b_0}{4} - \frac{b_2}{6} + \frac{b_4}{24}\right) + Cb_2 = g_2,$$
$$A\left(\frac{e_3}{24} - \frac{b_1}{128} + \frac{3b_3}{320} - \frac{b_5}{576} + \frac{b_7}{5760}\right) + B\left(\frac{b_1}{24} - \frac{b_3}{16} + \frac{b_5}{48}\right) + Cb_3 = g_3,$$
$$A\left(\frac{b_0}{192} - \frac{b_2}{128} + \frac{b_4}{480} - \frac{b_6}{1680} + \frac{b_8}{13\,440}\right) + B\left(\frac{b_2}{48} - \frac{b_4}{30} + \frac{b_6}{80}\right) + Cb_2 = g_4,$$

and for $4 < n \le N$,

$$A\left(\frac{b_{n-4}}{16n(n-1)(n-2)(n-3)} - \frac{b_{n-2}}{4(n+1)n(n-1)(n-3)} + \frac{3b_n}{8(n+2)(n+1)(n-1)(n-2)} \right.$$
$$\left. - \frac{b_{n+2}}{4(n+3)(n+1)n(n-1)} + \frac{b_{n+4}}{16(n+3)(n+2)(n+1)n} \right) + Cb_n = g_n.$$

Here $b_n = 0$ for $n > N$ and g_n are the Chebyshev series expansion coefficients for g. To obtain the equations that fix the last four coefficients, the boundary conditions, $w(\pm 1) = 0$ and $w_x(\pm 1) = 0$, are imposed. This gives the following equations

$$0 = e_0 \pm e_1 + \frac{e_2}{4} \mp \frac{e_3}{12} - \frac{7b_0}{192} \pm \frac{5b_1}{384} + \frac{47b_2}{1920} \mp \frac{9b_3}{640} - \frac{b_4}{160} \pm \frac{b_5}{1152} - \frac{b_6}{13\,440} \pm \frac{b_7}{5760} + \frac{b_8}{13\,440}$$
$$+ \sum_{n=5}^{N} (-1)^n \left(\frac{b_{n-4}}{16n(n-1)(n-2)(n-3)} - \frac{b_{n-2}}{4(n+1)n(n-1)(n-3)} + \frac{3b_n}{8(n+2)(n+1)(n-1)(n-2)} \right.$$
$$\left. - \frac{b_{n+2}}{4(n+3)(n+1)n(n-1)} + \frac{b_{n+4}}{16(n+3)(n+2)(n+1)n} \right)$$

and

$$0 = e_1 \pm e_2 + \frac{e_3}{4} \mp \frac{b_0}{12} - \frac{b_1}{24} \pm \frac{5b_2}{96} + \frac{3b_3}{64} \mp \frac{b_4}{120} - \frac{b_5}{192} \mp \frac{b_6}{480}$$
$$+ \sum_{n=4}^{N} (\pm 1)^n \left(\frac{b_{n-3}}{8n(n-1)(n-2)} - \frac{3b_{n-1}}{8(n+1)n(n-2)} + \frac{3b_{n+1}}{8(n+2)n(n-1)} - \frac{b_{n+3}}{8(n+2)(n+1)n} \right),$$

where again, $b_n = 0$ for $n > N$. These equations are in the matrix $\widehat{\boldsymbol{LBC2}}$ and vector $\widehat{\boldsymbol{RBC2}}$. Once the matrix system is solved, we can use the coefficients to find the functions and their derivatives using the truncated versions of Eqs. (3.23)–(3.27).

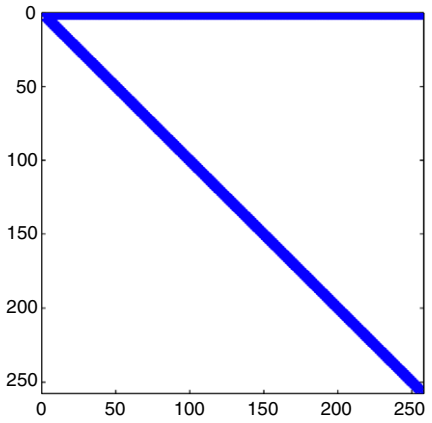

Fig. 3. Sparsity pattern of the discretized Chebyshev spectral space boundary value problem integration operator $\tilde{\boldsymbol{S}}^0+\tilde{\boldsymbol{S}}^2+\tilde{\boldsymbol{S}}^4+\widehat{\boldsymbol{LBC2}}$ with 257 Chebyshev modes, compare with Figs. 1, 2 and 4 for the other collocation Chebyshev methods studied here.

An important observation in this derivation is that, because the Chebyshev basis is a polynomial basis, the four integration constants, c_1, c_2x, c_3x^2 and c_4x^3 only involve combinations of the low order Chebyshev polynomials, and hence the integration matrices remain sparse. This is not true for a non-periodic function whose highest derivative is expanded in a Fourier series with lower order derivatives being obtained by integration.

Finally, in the preconditioned Chebyshev method, if the truncated expansion for $\hat{\boldsymbol{w}}$ has $N+1$ modes, then a $(N+1)\times(N+1)$ linear system is solved. In the Chebyshev integration method, four further equations are obtained because of the integration constants, thus if the truncated expansion for $\hat{\boldsymbol{w}}_{xxxx}$ has $N+1$ modes, then a $(N+5)\times(N+5)$ matrix system is solved. The typical sparsity pattern for the matrix obtained when using the Chebyshev integration method matrix is shown in Fig. 3 and is similar to the sparsity pattern obtained using the preconditioned Chebyshev differentiation method shown in Fig. 2(a) — in both cases the top four rows are full and there is a diagonal band.

3.1.4. The real space Chebyshev integration method

To construct a Chebyshev integration method which does not require the transformation of the forcing function into a Chebyshev series, we will follow El-Gendi [24] and transform the formulas found in Section 3.1.3 for how the integration matrices act on the coefficients for the Chebyshev expansion of a series, to formulas for matrices which act on the real space values of a function on Chebyshev–Gauss–Lobatto points. We will do this by using Clenshaw–Curtis quadrature to transform the expansions in Chebyshev polynomials to functions in real space evaluated at Chebyshev Gauss–Lobatto points. This gives a formulation of the Chebyshev integration method, which although it uses dense matrices, may form the basis for an integral formulation of the spectral element method introduced in [42] using the differentiation formulation. We could also use Gauss quadrature to formulate this method; this would give slightly more accurate results (see, for example, Trefethen [43]), but for consistency with the other discretizations which use Chebyshev Gauss–Lobatto points, we will stick to using these discretization points when formulating the real space integration matrices. This also has the advantage that quickly computable explicit formulas can be given for the resulting integration matrices. Our approach differs slightly from that used in [24] because it uses $(N+5)\times(N+5)$ matrices instead of $(N+1)\times(N+1)$ matrices. This allows us to calculate both the solution to the constant coefficient differential equation and derivatives of the solution to the constant coefficient differential equation for a wider variety of boundary conditions. We will not consider the modified implementations used in [36] because his numerical results do not show significant improvements over those of El-Gendi [24] and because none of the real space Chebyshev integration methods result in sparse matrices which is the important consideration for performing large simulations.

To formulate a real space integration method, we will use numerical integration to relate the Chebyshev coefficients to the function values of the highest derivative. Thus if

$$w_{xxxx}=\sum_{n=0}^{\infty}b_nT_n(x),$$

then using the orthogonality of the Chebyshev polynomials, we find that

$$b_n=\frac{2}{\pi c_n}\int_0^1 w_{xxxx}(x)T_n(x)\frac{1}{\sqrt{1-x^2}}\mathrm{d}x$$

where

$$c_n:=\begin{cases}2, & n=0,\\ 1, & \text{otherwise.}\end{cases}$$

We will evaluate these integrals using El-Gendi's [24] method, that is collocation and Clenshaw–Curtis quadrature. Our implementation will differ slightly from El-Gendi's so that it is easier to change the boundary conditions that are imposed.

The discrete collocation analog of the equations above is,

$$w_{xxxx} \approx \sum_{n=0}^{N} b_n T_n(x)$$

and

$$\begin{aligned} b_n &= \frac{2}{\bar{c}_n N} \sum_{i=0}^{N} \frac{1}{\bar{c}_i} w_{xxxx}(x_i) T_n(x_i) \\ &= \frac{2}{\bar{c}_n N} \sum_{i=0}^{N} \frac{1}{\bar{c}_i} w_{xxxx}(x_i) \cos\frac{n\pi i}{N}, \end{aligned} \tag{3.28}$$

where the x_i are the Chebyshev Gauss–Lobatto points and $\bar{c}_0 = \bar{c}_N = 2$ and $\bar{c}_n = 1$ for $1 \le n \le N-1$. Further information on the derivation of these relationships can be found in [44, p. 42].

Using these relationships for a truncation of the infinite Chebyshev expansion, we can rewrite Eqs. (3.23)–(3.27) in real space instead of Chebyshev spectral space. For the fourth order linear boundary value problem in Eq. (3.1), we find that the integration matrices can be re-arranged as follows,

$$w_{xxxx}(x_i) = \sum_{j=0}^{N} \delta_{i,j} w_{xxxx}(x_j), \tag{3.29}$$

where

$$\delta_{i,j} := \begin{cases} 1, & i = j \\ 0, & \text{otherwise,} \end{cases}$$

$$\begin{aligned} w_{xxx}(x_i) &= e_3 + \sum_{j=0}^{N} \frac{2}{N\bar{c}_j} w_{xxxx}(x_j) \left[\frac{1}{\bar{c}_0} T_0(x_j) T_1(x_i) + T_1(x_j) \frac{T_2(x_i)}{4} + T_2(x_j) \left(\frac{T_3(x_i)}{6} - \frac{T_1(x_i)}{2} \right) \right. \\ &\quad \left. + \sum_{n=3}^{N} \frac{1}{\bar{c}_n} T_n(x_j) \left(\frac{T_{n+1}(x_i)}{2(n+1)} - \frac{T_{n-1}(x_i)}{2(n-1)} \right) \right], \end{aligned} \tag{3.30}$$

$$\begin{aligned} w_{xx}(x_i) &= e_2 + e_3 T_1(x_i) + \sum_{j=0}^{N} \frac{2}{N\bar{c}_j} w_{xxxx}(x_j) \left[\frac{1}{\bar{c}_0} \frac{T_0(x_j) T_2(x_i)}{4} + T_1(x_j) \left(\frac{T_3(x_i)}{24} - \frac{T_1(x_i)}{8} \right) \right. \\ &\quad + T_2(x_j) \left(\frac{T_4(x_i)}{48} - \frac{T_2(x_i)}{6} \right) + \sum_{n=3}^{N} \frac{1}{\bar{c}_n} T_n(x_j) \left(\frac{T_{n+2}(x_i)}{4(n+2)(n+1)} - \frac{T_n(x_i)}{2(n+1)(n-1)} \right. \\ &\quad \left. \left. + \frac{T_{n-2}(x_i)}{4(n-2)(n-1)} \right) \right], \end{aligned} \tag{3.31}$$

$$\begin{aligned} w_x(x_i) &= e_1 + e_2 T_1(x_i) + e_3 \frac{T_2(x_i)}{4} + \sum_{j=0}^{N} \frac{2}{N\bar{c}_j} w_{xxxx}(x_j) \\ &\quad \times \left[\frac{1}{\bar{c}_0} T_0(x_j) \left(\frac{T_3(x_i)}{24} - \frac{T_1(x_i)}{8} \right) + T_1(x_j) \left(\frac{T_4(x_i)}{192} - \frac{T_2(x_i)}{24} \right) + T_2(x_j) \left(\frac{T_5(x_i)}{480} - \frac{T_3(x_i)}{32} + \frac{T_1(x_i)}{12} \right) \right. \\ &\quad + T_3(x_j) \left(\frac{T_6(x_i)}{960} - \frac{3T_4(x_i)}{320} + \frac{3T_2(x_i)}{64} \right) + \sum_{n=4}^{N} \frac{1}{\bar{c}_n} T_n(x_j) \left(\frac{T_{n+3}(x_i)}{8(n+3)(n+2)(n+1)} \right. \\ &\quad \left. \left. - \frac{3T_{n+1}(x_i)}{8(n+2)(n+1)(n-1)} + \frac{3T_{n-1}(x_i)}{8(n+1)(n-1)(n-2)} - \frac{T_{n-3}(x_i)}{8(n-1)(n-2)(n-3)} \right) \right] \end{aligned} \tag{3.32}$$

and

$$\begin{aligned} w(x_i) &= e_0 + e_1 T_1(x_i) + \frac{e_2}{4} T_2(x_i) + e_3 \left(\frac{T_3(x_i)}{24} - \frac{T_1(x_i)}{8} \right) + \sum_{j=0}^{N} \frac{2}{N\bar{c}_j} w_{xxxx}(x_j) \\ &\quad \times \left[\frac{1}{\bar{c}_0} T_0(x_j) \left(\frac{T_4(x_i)}{192} - \frac{T_2(x_i)}{24} \right) + T_1(x_j) \left(\frac{T_5(x_i)}{1920} - \frac{T_3(x_i)}{128} + \frac{T_1(x_i)}{48} \right) \right. \\ &\quad \left. + T_2(x_j) \left(\frac{T_6(x_i)}{5760} - \frac{T_4(x_i)}{240} + \frac{11T_2(x_i)}{384} \right) + T_3(x_j) \left(\frac{T_7(x_i)}{13\,440} - \frac{T_5(x_i)}{960} + \frac{3T_3(x_i)}{320} - \frac{3T_1(x_i)}{128} \right) \right. \end{aligned}$$

$$+T_4(x_j)\left(\frac{T_8(x_i)}{21\,504}-\frac{T_6(x_i)}{7140}+\frac{T_4(x_i)}{480}-\frac{T_2(x_i)}{120}\right)+\sum_{n=5}^{N}\frac{1}{\bar{c}_n}T_n(x_j)\left(\frac{T_{n+4}(x_i)}{16(n+4)(n+3)(n+2)(n+1)}\right.$$
$$-\frac{T_{n+2}(x_i)}{4(n+3)(n+2)(n+1)(n-1)}+\frac{3T_n(x_i)}{8(n+2)(n+1)(n-1)(n-2)}-\frac{T_{n-2}(x_i)}{4(n+1)(n-1)(n-2)(n-3)}$$
$$\left.+\frac{T_{n-4}(x_i)}{16(n-1)(n-2)(n-3)(n-4)}\right)\Bigg]. \tag{3.33}$$

A further four equations are obtained from the boundary conditions, $w(\pm1)=0$ and $w_x(\pm1)=0$, these are

$$0=e_0\pm e_1+\frac{e_2}{4}\mp\frac{e_3}{12}+\sum_{j=0}^{N}\frac{2}{N\bar{c}_j}w_{xxxx}(x_j)\Bigg[-\frac{1}{\bar{c}_0}\frac{1}{12}T_0(x_j)\pm\frac{13}{960}T_1(x_j)+\frac{71}{2880}T_2(x_j)\mp\frac{101}{6720}T_3(x_j)$$
$$-\frac{773}{121856}T_4(x_j)+\sum_{n=5}^{N}\frac{1}{\bar{c}_n}(\pm1)^n\frac{105}{(n^2-16)(n^2-9)(n^2-4)(n^2-1)}T_n(x_j)\Bigg] \tag{3.34}$$

and

$$0=e_1\pm e_2+\frac{e_3}{4}+\sum_{j=0}^{N}\frac{2}{N\bar{c}_j}w_{xxxx}(x_j)\Bigg[\mp\frac{1}{\bar{c}_0}\frac{1}{12}T_0(x_j)-\frac{7}{192}T_1(x_j)\pm\frac{1}{480}T_2(x_j)+\frac{37}{960}T_3(x_j)$$
$$-\sum_{n=4}^{N}(\pm1)^{n+1}\frac{1}{\bar{c}_n}\frac{15}{(n^2-9)(n^2-4)(n^2-1)}T_n(x_j)\Bigg]. \tag{3.35}$$

We note that Eq. (3.29) is an $(N+1)\times(N+1)$ identity matrix, with the further four rows and four columns of the $(N+5)\times(N+5)$ matrix which are used to enforce the boundary conditions being zero. In the implementation used here, we choose to place these rows and columns in the top four rows and first four columns of the matrix. The other matrices given in Eqs. (3.30)–(3.33) are full matrices, with the top four rows empty and the first four columns partially empty depending on the number of boundary conditions that need to be enforced — the sparsity patterns for these matrices are shown in Fig. 4. The resulting system of equations for approximating the solution to Eq. (3.1) is given by

$$\left(A\boldsymbol{I}^4+B\boldsymbol{I}^2+C\boldsymbol{I}^0+\boldsymbol{LBC3}\right)\boldsymbol{w}_{xxxx}=\boldsymbol{g}+\boldsymbol{RBC3}, \tag{3.36}$$

where $\boldsymbol{I}^k$ denotes the kth order integration matrix, ***LBC3*** is a matrix containing Eqs. (3.34) and (3.35) which enforce the values of the boundary conditions specified in the first four entries of the array ***RBC3***. We note that the entries for $\boldsymbol{I}^0$ can be found from Eq. (3.29), the entries for $\boldsymbol{I}^1$ from Eq. (3.30), the entries for $\boldsymbol{I}^2$ from Eq. (3.31), the entries for $\boldsymbol{I}^3$ from Eq. (3.32) and the entries for $\boldsymbol{I}^4$ can be found from Eq. (3.33). In all cases the top four rows of the matrices are reserved for the boundary conditions and the entry in column j and row $i+4$ is given by setting i and j in these expressions and summing over n.

Constructing these integration matrices using Eqs. (3.29)–(3.35) directly as indicated in the previous paragraph requires $O(N^3)$ operations and has a very poor memory access pattern. Driscoll [45,37] has observed that the matrices can be calculated efficiently by constructing Chebyshev forward and backward transform matrices, which we denote by $\boldsymbol{CT}$ and $\boldsymbol{CT}^{-1}$ respectively. The entries for $\boldsymbol{CT}$ can be found from the discrete Chebyshev transform on Gauss–Lobatto points given in Eq. (3.28), and the entries in $\boldsymbol{CT}^{-1}$ can be found from

$$w_{xxxx}(x_i)=\sum_{n=0}^{N}b_n\cos\frac{n\pi i}{N}.$$

Thus, $\boldsymbol{I}^4\approx(\boldsymbol{CT}^{-1})(\hat{\boldsymbol{S}}^4)(\boldsymbol{CT})$, where $\hat{\boldsymbol{S}}^4$ is defined in Eq. (3.27). We do not quite get equality because the matrices are not the same size since the equations for the boundary conditions are treated slightly differently in real space compared to Chebyshev spectral space. Equality does hold for the sub matrix of $(N+1)\times(N+1)$ entries which are not directly related to the boundary conditions, that is

$$\boldsymbol{I}^4(5:N+5,5:N+5)=\left(\boldsymbol{CT}^{-1}\right)\hat{\boldsymbol{S}}(5:N+5,5:N+5)\,(\boldsymbol{CT})\,.$$

3.2. Numerical results

This section contains a numerical comparison of the accuracy in the L^2 and $W^{2,2}$ norms of the previously described Chebyshev methods for solving two linear boundary value problems. There are several methods of implementing the Chebyshev method in spectral space. Coutsias et al. [17] describe one variation of the Chebyshev integration method in which solutions of the homogeneous boundary value problem are added to a particular solution of the inhomogeneous boundary value problem. When solving the linear system for the Chebyshev integration method in the numerical comparison that follows, a solution which satisfies all the boundary conditions is obtained. This is because for the linear boundary value problems considered here, the modification examined in [17] do not affect the accuracy of the numerical solutions that are

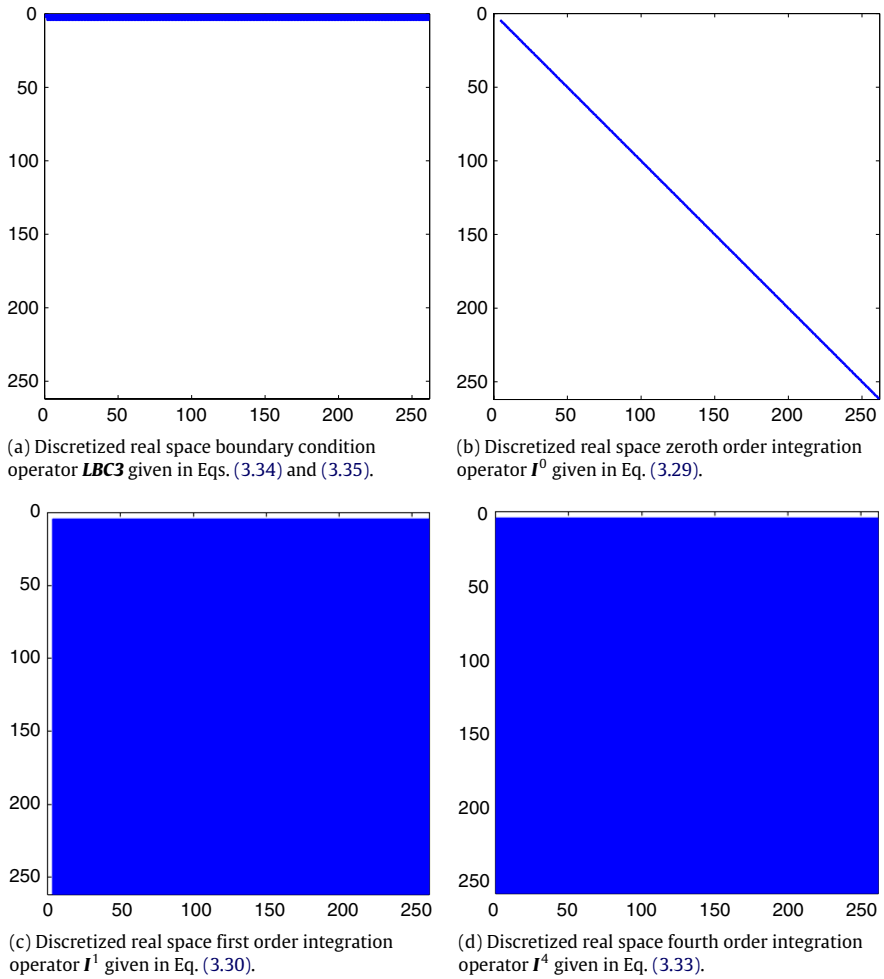

(a) Discretized real space boundary condition operator ***LBC3*** given in Eqs. (3.34) and (3.35).

(b) Discretized real space zeroth order integration operator $\boldsymbol{I}^0$ given in Eq. (3.29).

(c) Discretized real space first order integration operator $\boldsymbol{I}^1$ given in Eq. (3.30).

(d) Discretized real space fourth order integration operator $\boldsymbol{I}^4$ given in Eq. (3.33).

Fig. 4. Sparsity patterns with 257 collocation points for the real space Chebyshev integration method, compare with Figs. 1–3 for the other collocation Chebyshev methods studied here.

obtained. Numerical comparisons of the accuracy of approximate derivatives of the solution obtained by the preconditioned Chebyshev differentiation method calculated using the Fast Fourier Transform and calculated using spectral differentiation matrices are included, because in this case the results differ. Calculations in this section were done using MATLAB 7.3 running on a laptop with a 2 GHz Intel Core Duo processor and 2 Gb of RAM. MATLAB's backslash was used to obtain solutions to the resulting linear systems of equations.

We examine numerical approximations to the following two boundary value problems for $x \in [-1, 1]$ with the associated boundary conditions and given exact solutions,

$$\begin{aligned} &w_{xxxx} + 2w_{xx} + w = \cos(x), \\ &w(-1) = 0, \qquad w(1) = 0, \qquad w_x(-1) = 0, \qquad w_x(1) = 0, \\ &w(x) = \frac{4x\cos^2(1)\sin(x) - \cos(x)\left\{\sin(2) - 2 + x^2\left[2 + \sin(2)\right]\right\}}{8\left[2 + \sin(2)\right]}, \end{aligned} \tag{3.37}$$

and

$$\begin{aligned} &50^{-4} w_{xxxx} - w = 10, \\ &w(-1) = 0, \qquad w(1) = 0, \qquad w_x(-1) = 0, \qquad w_x(1) = 0, \\ &w(x) = \frac{10\sinh(50)\cos(50x) + 10\sin(50)\cosh(50x)}{\sin(50)\cosh(50) + \sinh(50)\cos(50)} - 10. \end{aligned} \tag{3.38}$$

The exact solutions are plotted in Figs. 5 and 8.

Figs. 6, 7, 9 and 10 show the convergence of numerical solutions to these linear boundary value problems obtained using Chebyshev differentiation, preconditioned Chebyshev differentiation and Chebyshev integration methods respectively.

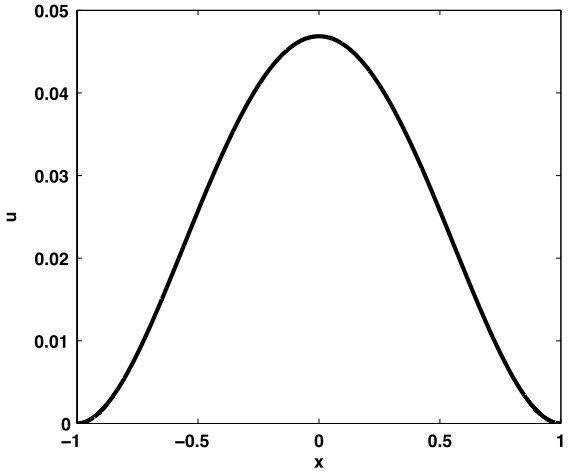

Fig. 5. Exact solution to Eq. (3.37).

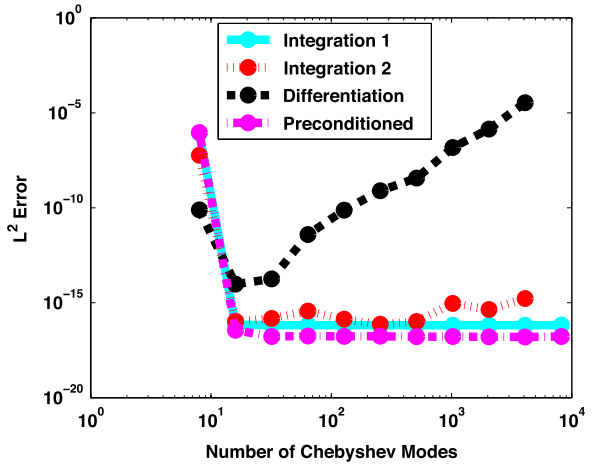

Fig. 6. Convergence in L^2 norm for Eq. (3.37). In the legend, Integration 1 — spectral space Chebyshev integration method ; Integration 2 — real space Chebyshev integration method; Differentiation — real space collocation differentiation method; Preconditioned — spectral space Chebyshev preconditioned differentiation method.

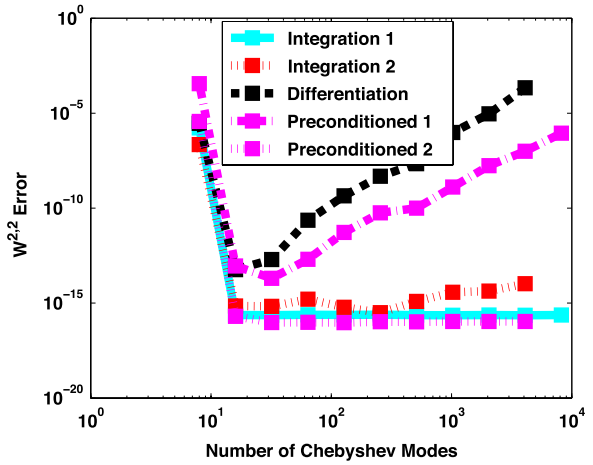

Fig. 7. Convergence in $W^{2,2}$ norm for Eq. (3.37). In the legend, Integration 1 — spectral space Chebyshev integration method; Integration 2 — real space Chebyshev integration method; Differentiation — real space collocation differentiation method; Preconditioned 1 — spectral space Chebyshev preconditioned differentiation method with derivatives obtained using spectral differentiation matrices; and Preconditioned 2 — spectral space preconditioned Chebyshev differentiation method with derivatives obtained using the Fast Fourier Transform.

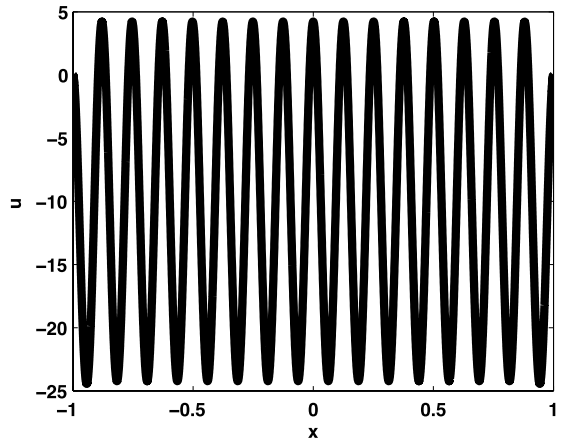

Fig. 8. Exact solution to Eq. (3.38).

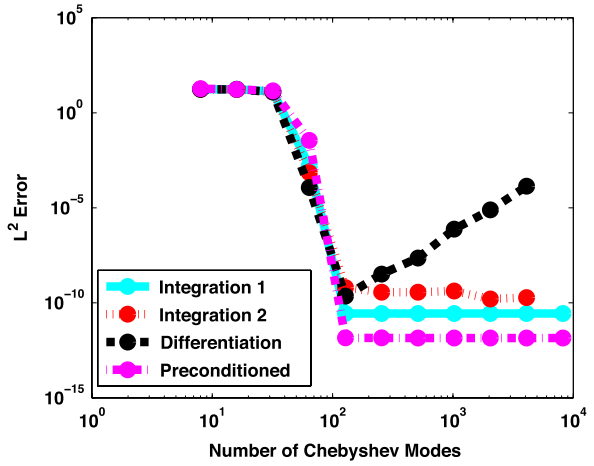

Fig. 9. Convergence in the L^2 norm for Eq. (3.38). In the legend, Integration 1 — spectral space Chebyshev integration method; Integration 2 — real space Chebyshev integration method; Differentiation — real space collocation differentiation method; Preconditioned — spectral space Chebyshev preconditioned differentiation method.

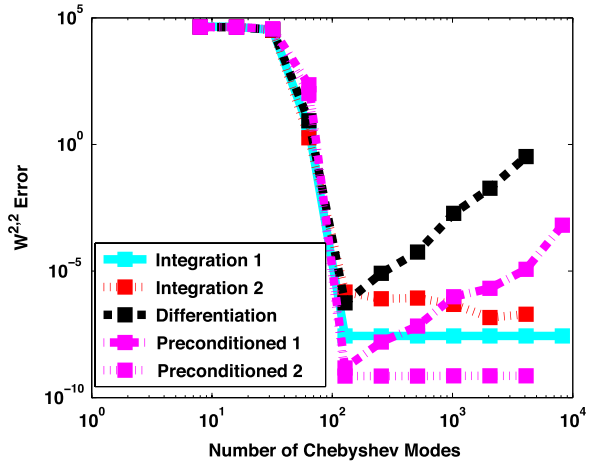

Fig. 10. Convergence in the $W^{2,2}$ norm for Eq. (3.38). In the legend, Integration 1 — spectral space Chebyshev integration method; Integration 2 — real space Chebyshev integration method; Differentiation — real space collocation differentiation method; Preconditioned 1 — spectral space Chebyshev preconditioned differentiation method with derivatives obtained using spectral differentiation matrices; and Preconditioned 2 — spectral space Chebyshev preconditioned differentiation method with derivatives obtained using the Fast Fourier Transform.

Trefethen and Trummer [20] have shown that using large real space Chebyshev differentiation matrices in numerical calculations gives results that are sensitive to errors introduced by finite precision arithmetic. The figures show results using as many modes as could be used with the available amount of memory. Trefethen and Trummer [20] also note that differentiation of the Chebyshev interpolant of a function using the Fast Fourier Transform is sensitive to errors introduced by finite precision arithmetic, thus the numerical instability observed here cannot be alleviated by this method of calculating derivatives. Greengard [25] showed that, provided the resulting linear systems are solved accurately, by using an integration matrix formulation the numerical instabilities that occur when obtaining the solution and derivatives of the solution to two-point boundary value problems are avoided. The figures confirm these previous results when extended to fourth order boundary value problems and show that the real space Chebyshev differentiation matrix method is a poor method when a large number of modes are used in both L^2 and $W^{2,2}$ norms. The preconditioned Chebyshev differentiation method is a good method when accurate results in the L^2 norm are required. If derivatives are obtained using the Fast Fourier Transform, the preconditioned Chebyshev method is a poor method to use when accurate approximations of the derivative are required. Finally, the figures show that accurate results in the $W^{2,2}$ norm can be obtained using the preconditioned Chebyshev differentiation method when derivatives are found using spectral differentiation matrices in spectral space. As explained in [10, p. 220], the reason for the difference in the accuracy of real space differentiation and spectral space differentiation is that, even though both differentiation matrices are ill conditioned, the accurately computed spectral expansion coefficients decay sufficiently rapidly to ensure that when they are multiplied by the spectral differentiation matrices, the results remain accurate. If the Fast Fourier Transform is used to calculate the spectral expansion coefficients, a computational error is introduced which is then amplified upon differentiation (see Higham [46, p. 451] for an analysis of errors introduced by a simple Fast Fourier Transform algorithm).

The Chebyshev integration method uses more modes, $N + 5$, as opposed to $N + 1$ for the preconditioned Chebyshev differentiation method. Canuto et al. [16, p. 177] suggest that the Chebyshev integration method should be more accurate than the preconditioned Chebyshev differentiation method because it has more degrees of freedom. It is therefore surprising that the Chebyshev integration method is slightly less accurate than the preconditioned Chebyshev differentiation method when more than 100 modes are used. Figs. 9 and 10 show that the preconditioned Chebyshev differentiation method is less accurate when there are less than 100 modes, because here the extra degrees of freedom give better resolution. When more than 100 modes are used, the preconditioned method seems to give a matrix which can be solved more accurately. As we have not done a full error analysis of the solution procedure used by MATLAB's backslash for these matrix systems, we do not have a proof which explains this difference in accuracy. As explained in [46, p. 120] it is likely that since the preconditioned and Chebyshev integration linear systems have similar matrix structures, the faster decay of the terms on the right hand side, $\widehat{\boldsymbol{PD}}^0\hat{\boldsymbol{f}}$ in Eq. (3.7) as opposed to $\hat{\boldsymbol{f}}$ in Eq. (3.22), makes it easier to solve the preconditioned matrix system more accurately than the Chebyshev integration matrix system.

4. Initial boundary value problems

In this section, the performance of an IMEX time stepping scheme that uses the Chebyshev integration method and preconditioned Chebyshev differentiation methods to solve semilinear initial boundary value problems is examined. The accuracy and computational cost of two different implementations of the Chebyshev integration method and of the preconditioned Chebyshev differentiation method for IMEX time stepping schemes are compared. The modification made to the Chebyshev integration method is to combine a particular solution of the inhomogeneous boundary value problem solved at each time step to solutions of the homogeneous boundary value problem pre-solved before time stepping began so that as suggested in [17], only a banded and not a bordered banded linear system is solved at each time step. The comparison also includes a fully implicit time stepping scheme using the Chebyshev integration spatial discretization. This section ends with an example of a semilinear equation with a stiff nonlinear term for which only the fully implicit scheme was stable.

4.1. An implicit–explicit temporal discretization

A simple second order time stepping scheme is constructed for the equation

$$\rho w_{tt} - \beta w_{xxt} = \gamma^2 \left(w_x^3 - w_x\right)_x - \epsilon^2 w_{xxxx}, \tag{4.1}$$

where $x \in [-1, 1]$ and $t \in [0, 1]$ are the spatial and temporal variables, and ρ, β, γ and ϵ are real positive constants. This equation is used as a simplified dynamic model for phase transformations and has an exact traveling wave solution obtained in [47] which we rewrite as

$$w(x,t) = \sqrt{2}\frac{\epsilon}{\gamma}\log\left\{\cosh\left[\frac{\kappa x - \omega t}{\kappa^2}\sqrt{\frac{\omega^2}{2\epsilon^2}\left(\rho - \frac{\beta^2}{6\epsilon^2}\right) + \frac{\gamma^2\kappa^2}{2\epsilon^2}}\right]\right\} - \frac{\omega\beta(\kappa x - \omega t)}{3\kappa^2\sqrt{2}\epsilon}. \tag{4.2}$$

In this solution, κ is the wavenumber and ω is the wave frequency. The boundary conditions, $w(-1, t)$, $w(1, t)$, $w_x(-1, t)$ and $w_x(1, t)$, and initial conditions $w(x, 0)$ and $w_t(x, 0)$ are obtained from this exact solution. Since single domain spectral collocation methods cannot approximate discontinuous functions well, only smooth solutions are used for the numerical

comparison, for which the inequality, $\omega^2(\rho - \beta^2/6\epsilon^2) + \gamma^2\kappa^2 \geq 0$, must hold since if it does not, the exact solution in Eq. (4.2) is discontinuous as the hyperbolic cosine of a purely imaginary function is actually the cosine of the magnitude of the purely imaginary function, and the cosine can be zero for which the logarithm is undefined.

To construct a second order IMEX time stepping scheme, time dependent terms are discretized using second order finite difference approximations centered at the next time step. This is done using second order backward differentiation approximations for the terms w_{tt} and w_{xxt}, and an Adams–Bashforth or forward extrapolation method for the nonlinear term $(w_x^3 - w_x)_x$. The resulting time stepping scheme is

$$\begin{aligned}&\frac{\rho}{\delta t^2}\left(2w^{j+1} - 5w^j + 4w^{j-1} - w^{j-2}\right) - \frac{\beta}{2\delta t}\left(3w_{xx}^{j+1} - 4w_{xx}^j + w_{xx}^{j-1}\right)\\ &\quad = 2\gamma^2\left[(w_x^j)^3 - w_x^j\right]_x - \gamma^2\left[(w_x^{j-1})^3 - w_x^{j-1}\right]_x - \epsilon^2 w_{xxxx}^{j+1}.\end{aligned} \tag{4.3}$$

In this equation, the superscript on w denotes the time step at which the function is evaluated. Eq. (4.3) is rearranged to obtain the new iterate w^{j+1} in terms of the previous three iterates w^j, w^{j-1} and w^{j-2}

$$\begin{aligned}\frac{2\rho}{\delta t^2}w^{j+1} - \frac{3\beta}{2\delta t}w_{xx}^{j+1} + \epsilon^2 w_{xxxx}^{j+1} = &\frac{\rho}{\delta t^2}\left(5w^j - 4w^{j-1} + w^{j-2}\right) - \frac{\beta}{2\delta t}\left(4w_{xx}^j - w_{xx}^{j-1}\right)\\ &+ 2\gamma^2\left[(w_x^j)^3 - w_x^j\right]_x - \gamma^2\left[(w_x^{j-1})^3 - w_x^{j-1}\right]_x.\end{aligned} \tag{4.4}$$

This shows that at each time step, a linear boundary value problem is solved and so the Chebyshev integration method can be used.

The implementations of Chebyshev integration methods in IMEX time stepping schemes in the literature differ (see, for example, Coutsias et al. [17], Cox and Matthews [28] and Lundbladh et al. [29]). For completeness, a description of the implementation of the numerical scheme in Eq. (4.4) using the Chebyshev integration method is now provided. A similar approach is used for the spectral space preconditioned Chebyshev differentiation method and so this is not included. The highest spatial derivative term in Eq. (4.4) is approximated by a truncated Chebyshev series, $w_{xxxx}^j \approx \sum_{n=0}^N a_n^j T_n(x)$. Lower derivative approximations are found by integration. The sum of the terms in the scheme in Eq. (4.4) that were computed in the previous three time steps in Chebyshev spectral space is stored in the vector $\hat{\boldsymbol{g}}^j$ which is defined as

$$\hat{\boldsymbol{g}}^j := \frac{\rho}{\delta t^2}\left(5\hat{\boldsymbol{w}}^j - 4\hat{\boldsymbol{w}}^{j-1} + \hat{\boldsymbol{w}}^{j-2}\right) - \frac{\beta}{2\delta t}\left(4\hat{\boldsymbol{w}}_{xx}^j - \hat{\boldsymbol{w}}_{xx}^{j-1}\right) + 2\gamma^2\left[3\widehat{(\boldsymbol{w}_x^j)^2\boldsymbol{w}_{xx}^j} - \hat{\boldsymbol{w}}_{xx}^j\right] - \gamma^2\left[3\widehat{(\boldsymbol{w}_x^{j-1})^2\boldsymbol{w}_{xx}^{j-1}} - \hat{\boldsymbol{w}}_{xx}^{j-1}\right],$$

where the vectors $\hat{\boldsymbol{w}}^j$ and $\hat{\boldsymbol{w}}_{xx}^j$ are the vectors of coefficients of the truncated Chebyshev polynomials which approximate the solution and its second derivative at the jth time step. The vectors w_x^j, and w_{xx}^j are the real space approximations to w_x and w_{xx} at the jth time step at the $N+1$ collocation grid points. The nonlinear term, $3\left(w_x^j\right)^2 w_{xx}^j - w_{xx}^j$, is projected onto the space of $N+1$ Chebyshev polynomials by using a Fast Fourier Transform, see, for example, Trefethen [41, p. 75]. In doing so, aliasing errors are ignored. Aliasing errors occur because the multiplication of the finite dimensional approximation of $\widehat{(\boldsymbol{w}_x^j)^2\boldsymbol{w}_{xx}^j}$ produces components with higher frequencies than are originally in the original finite dimensional approximations of $\hat{\boldsymbol{w}}_x^j$ and $\hat{\boldsymbol{w}}_{xx}^j$. However, if the solution is sufficiently well resolved, then the coefficients for the high frequency components are small and the finite dimensional approximation of $w_x^2 w_{xx}$ using the same number of Chebyshev polynomials as the finite dimensional approximation of w_x and w_{xx} will also be accurate, see Canuto et al. [16, p. 163]. A sparse, bordered banded system of equations,

$$\hat{\boldsymbol{L}}\hat{\boldsymbol{w}}_{xxxx}^{j+1} = \hat{\boldsymbol{g}}^j + \widehat{\boldsymbol{RBC2}}^{j+1}, \tag{4.5}$$

where

$$\hat{\boldsymbol{L}} := \epsilon^2\hat{\boldsymbol{S}}^0 - \frac{3\beta}{2\delta t}\hat{\boldsymbol{S}}^2 + \frac{2\rho}{\delta t^2}\hat{\boldsymbol{S}}^4 + \widehat{\boldsymbol{LBC2}},$$

is then obtained. In these equations: $\hat{\boldsymbol{w}}_{xxxx}^{j+1}$ is the vector of coefficients of the Chebyshev polynomials which approximate the solution of the fourth derivative at the jth time step; $\hat{\boldsymbol{g}}^j$ is a vector with entries g_n^j; the matrices $\hat{\boldsymbol{S}}^0$, $\hat{\boldsymbol{S}}^2$ and $\hat{\boldsymbol{S}}^4$ are the zeroth, second and fourth order integration matrices; $\widehat{\boldsymbol{LBC2}}$ is a matrix formed from the equations for the boundary conditions; and $\widehat{\boldsymbol{RBC2}}^{j+1}$ is a vector with the values of the boundary conditions.

In typical implementations of time stepping schemes, Eq. (4.4) is multiplied by δt^2. Here by not doing so, the smallest non-zero matrix entries in $\hat{\boldsymbol{S}}^4$ do not become too small relative to the entries in $\epsilon^2\hat{\boldsymbol{S}}^0$. Finally, if ϵ^2 is small, because it multiplies the term $\hat{\boldsymbol{S}}^0$ which has non-zero entries that are of order one, the linear system can still be solved accurately using finite precision floating point arithmetic.

At each time step, the sparse linear system given by Eq. (4.5) is solved and used to advance in time in the space of Chebyshev polynomials. It is important to note that, for the linear operator $\hat{\boldsymbol{L}}$ in Eq. (4.5) used in this implicit time step to be invertible, it must include the integration matrix for the highest derivative term, $\hat{\boldsymbol{S}}^0$. This is because only the combination

$\hat{\boldsymbol{S}}^0 + \widehat{\boldsymbol{LBC2}}$ has full rank. Thus the integration matrix formulation as described here cannot be used in an explicit time stepping scheme. Coutsias et al. [17] explain that, it is possible to restrict the linear operator to a subspace where it is invertible, which would allow an explicit time stepping scheme to be used. However, stability constraints make explicit time stepping schemes unattractive for the numerical solution of stiff problems that occur in models for phase transformations with a fourth order spatial derivative.

When solving a system arising from the Chebyshev integration method with different right hand sides repeatedly, as is done in IMEX time stepping, Coutsias et al. [17] suggest that it may be faster to pre-solve a homogeneous boundary value problem first to obtain a set of solutions which can then be added to satisfy a variety of boundary conditions. This is because at each time step one can then solve a well conditioned banded diagonal matrix system. The particular solution of the well conditioned inhomogeneous boundary value problem does not satisfy the boundary conditions because the top four rows of the matrix are chosen to simplify the structure of the matrix. To satisfy the boundary conditions, solutions of the homogeneous boundary value problem are added to a particular solution of the inhomogeneous boundary value problem. Cox and Matthews [28] have implemented a variant of this method using analytic solutions for the homogeneous boundary value problem when solving the Navier–Stokes equations but, possibly unaware of [17] results, did not choose the matrices that are inverted to solve the inhomogeneous boundary value problem to have a banded structure. Lundbladh et al. [29] use two different particular solutions to the inhomogeneous boundary value problem and take a linear combination of these to satisfy the boundary values. As explained in [28], Lundbladh et al.'s method requires more computations, because two linear systems are solved at each time step instead of just one.

When using the Chebyshev integration method to do time stepping, as indicated in Eq. (4.4), a linear boundary value problem is solved at each time step. This can be done in several ways, which change the structure of the linear system that is solved. If a matrix system which contains the full equations for the boundary conditions is solved at each time step, a bordered banded system is obtained. As explained in [17], to solve a banded matrix system at each time step, one first pre-solves the linear boundary value problem in Eq. (4.4) with a right hand side that is zero. Four independent solutions to the homogeneous problem,

$$\epsilon^2 w^{hi}_{xxxx} - \frac{3\beta}{2\delta t} w^{hi}_{xx} + \frac{2\rho}{\delta t^2} w^{hi} = 0, \tag{4.6}$$

where i can be equal to 1, 2, 3 or 4, are then obtained. The four corresponding sets of boundary conditions are

$$w^{h1}(-1) = 1, \quad w^{h1}(1) = 0, \quad w^{h1}_{xx}(-1) = 0, \quad w^{h1}_{xx}(1) = 0, \tag{4.7}$$

$$w^{h2}(-1) = 0, \quad w^{h2}(1) = 1, \quad w^{h2}_{xx}(-1) = 0, \quad w^{h2}_{xx}(1) = 0, \tag{4.8}$$

$$w^{h3}(-1) = 0, \quad w^{h3}(1) = 0, \quad w^{h3}_{xx}(-1) = 1, \quad w^{h3}_{xx}(1) = 0, \tag{4.9}$$

$$w^{h4}(-1) = 0, \quad w^{h4}(1) = 0, \quad w^{h4}_{xx}(-1) = 0, \quad w^{h4}_{xx}(1) = 1. \tag{4.10}$$

These solutions can either be computed numerically, as suggested in [17], or analytically, as suggested in [28] before time stepping begins. To obtain the particular solution to Eq. (4.4), the first four diagonal entries in the matrix that are used to fix the boundary conditions, $\widehat{\boldsymbol{LBC2}}$ in Eq. (4.5), are set to be one. All other entries in these rows are zero. Similarly, the four entries for the boundary conditions in the right hand side vector $\widehat{\boldsymbol{RBC2}}^{j+1}$ in Eq. (4.5) are set to zero.

In the numerical examples computed using the bordered banded matrices, the matrix systems were solved by the sparse LU factorization implemented in MATLAB. The banded linear systems were also solved by a sparse LU factorization using MATLAB's backslash, but the default settings were changed to ensure that a band solver was used. Other solvers such as KLU and UMFPACK 5.0.2 (this is a slightly newer version of UMFPACK than that which is installed in MATLAB 7.3) which are part of [48] were also tested and found to give similar results. Since the best sparse solution method is architecture and solver setting dependent, we have not done an extensive numerical comparison of sparse solvers. An introduction to numerical methods for solving sparse linear systems can be found in [49].

In starting the multi-step time stepping scheme, the starting values $\boldsymbol{w}^0$, $\boldsymbol{w}^{-1}$ and $\boldsymbol{w}^{-2}$, need to be obtained. The initial conditions give $\boldsymbol{w}^0$ and $\boldsymbol{w}^0_t$. To obtain $\boldsymbol{w}^{-1}$ and $\boldsymbol{w}^{-2}$, we follow Kress [50] and use a Taylor expansion, the initial velocity and the partial differential equation, Eq. (4.1), to extrapolate backwards in time and still have $O(\delta t^2)$ accuracy. Thus,

$$\boldsymbol{w}^{-1} := \boldsymbol{w}^0 - \delta t \boldsymbol{w}^0_t + \frac{\delta t^2}{2} \boldsymbol{w}^0_{tt} \tag{4.11}$$

and

$$\boldsymbol{w}^{-2} := \boldsymbol{w}^0 - 2\delta t \boldsymbol{w}^0_t + \frac{(2\delta t)^2}{2} \boldsymbol{w}^0_{tt}. \tag{4.12}$$

The initial acceleration, $\boldsymbol{w}^0_{tt}$, is not given explicitly by the initial conditions, but by differentiating the initial conditions $\boldsymbol{w}^0$ and $\boldsymbol{w}^0_t$ with respect to x, $\boldsymbol{w}^0_x$, $\boldsymbol{w}^0_{xxxx}$ and $\boldsymbol{w}^0_{xxt}$ can be calculated and then the partial differential equation can be used to get

$$\boldsymbol{w}^0_{tt} = \rho^{-1} \left\{ \beta \boldsymbol{w}^0_{xxt} + \gamma^2 \left[(\boldsymbol{w}^0_x)^3 - \boldsymbol{w}^0_x \right]_x - \epsilon^2 \boldsymbol{w}^0_{xxxx} \right\}. \tag{4.13}$$

This can then be substituted into Eqs. (4.11) and (4.12) to calculate $\boldsymbol{w}^{-1}$ and $\boldsymbol{w}^{-2}$ so that a second order accurate numerical approximation of the true solution can be calculated.

4.2. A fully implicit temporal discretization

Time stepping schemes for variational problems that nearly conserve momenta (linear and angular) or nearly conserve energy are often used in computational solid mechanics where it is expected that dissipation is small. Reviews of these methods can be found in [51–56, p. 204]. In most solid mechanics applications, explicit time integration schemes are used because it can be computationally costly to solve equations that arise in fully implicit schemes. Here, a fully implicit scheme is used because stiff nonlinear and higher order capillarity terms make explicit and IMEX schemes unstable for practical time steps. Note that, because a Chebyshev spatial discretization is used, a full analysis of the scheme would show that it is variational in a weighted energy space. However, because well resolved spectral spatial discretizations give very accurate approximations of analytic solutions, it is expected that the scheme will retain the good energy dissipation properties that variational integration schemes have.

To introduce a stiff nonlinear term, we consider the equation,

$$\rho w_{tt} - \beta \left[w_{xt}\left(1 + w_x^2\right)\right]_x = \gamma^2 \left(w_x^3 - w_x\right)_x - \epsilon^2 w_{xxxx} + f(x,t), \tag{4.14}$$

for $x \in [-1, 1]$ and $t \in [0, 1]$. The forcing function, $f(x,t)$, the initial and the boundary conditions are chosen so that Eq. (4.14) has the exact solution

$$w = \sin(6\pi x t). \tag{4.15}$$

The dissipation term in Eq. (4.14),

$$\left[w_{xt}\left(1 + w_x^2\right)\right]_x,$$

differs from that in Eq. (4.1) because it is nonlinear. This unusual dissipation term is chosen because in frame indifferent viscoelastic models, the dissipation term in Lagrangian coordinates is also nonlinear (see, for example, Lew [54] and Lew et al. [55]).

Eq. (4.14) is approximated using the following temporal discretization,

$$\begin{aligned}
&\rho \frac{w^{j+1} - 2w^j + w^{j-1}}{\delta t^2} - \beta \frac{w_{xx}^{j+1} - w_{xx}^{j-1}}{2\delta t}\left[1 + \left(w_x^j\right)^2\right] - \beta \frac{w_x^{j+1} - w_x^{j-1}}{2\delta t}\left(2w_x^j\right) w_{xx}^j \\
&= \frac{\gamma^2}{2}\left[\left(\frac{w_x^{j+1} + w_x^j}{2}\right)^3 - \left(\frac{w_x^{j+1} + w_x^j}{2}\right)\right]_x + \frac{\gamma^2}{2}\left[\left(\frac{w_x^j + w_x^{j-1}}{2}\right)^3 - \left(\frac{w_x^j + w_x^{j-1}}{2}\right)\right]_x \\
&\quad - \frac{\epsilon^2}{4}\left(w_{xxxx}^{j+1} + 2w_{xxxx}^j + w_{xxxx}^{j-1}\right) + f\left(x, t^j\right).
\end{aligned} \tag{4.16}$$

This time discretization can be obtained by approximating the Lagrange–D'Alembert variational principle using the generalized midpoint rule, see Kane et al. [52], Lew [54] and Marsden and West [56] for further details. An error analysis using finite difference approximations in time at w^j can be used to show that this scheme is second order accurate.

A measure of the accuracy of the scheme is to check how well it conserves energy. Testing Eq. (4.14) with w_t and integrating by parts in space and then integrating in time from $t = 0$ to $t = T$, we find that

$$\begin{aligned}
&\int_{-1}^{1} \frac{\rho}{2} w_t^2(t = T) + \frac{\gamma^2}{4}\left[w_x^2(t = T) - 1\right]^2 + \frac{\epsilon^2}{2} w_{xx}^2(t = T)\mathrm{d}x \\
&\quad - \int_{-1}^{1} \frac{\rho}{2} w_t^2(t = 0) + \frac{\gamma^2}{4}\left[w_x^2(t = 0) - 1\right]^2 + \frac{\epsilon^2}{2} w_{xx}^2(t = 0)\mathrm{d}x \\
&= \int_0^T \int_{-1}^{1} -\beta w_{xt}^2\left(1 + w_x^2\right) + w_t f \mathrm{d}x + \gamma^2 (w_x^3 - w_x) w_t \,|_{x=-1}^{1} \\
&\quad - \epsilon^2 w_{xxx} w_t \,|_{x=-1}^{1} + \epsilon^2 w_{xx} w_{xt}|_{x=-1}^{1} \mathrm{d}t.
\end{aligned} \tag{4.17}$$

The corresponding discrete energy equality from which Eq. (4.16) is obtained, is found by approximating the terms on the left of Eq. (4.17) by

$$w_t \approx \frac{w^{j+1} - w^j}{\delta t}, \qquad w_x \approx \frac{w_x^{j+1} + w_x^j}{2} \quad \text{and} \quad \qquad w_{xx} \approx \frac{w_{xx}^{j+1} + w_{xx}^j}{2}.$$

The terms on the right of Eq. (4.17) are approximated by

$$w_t \approx \frac{w^{j+1} - w^{j-1}}{2\delta t} \quad \text{and} \quad w_{xt} \approx \frac{w_x^{j+1} - w_x^{j-1}}{2\delta t}.$$

Thus, the discrete energy equality is

$$\begin{aligned}
&\int_{-1}^{1}\frac{\rho}{2}\left(\frac{w^{j+1}-w^{j}}{\delta t}\right)^{2}+\frac{\gamma}{4}\left[\left(\frac{w_x^{j+1}+w_x^{j}}{2}\right)^{2}-1\right]^{2}+\frac{\epsilon^{2}}{2}\left(\frac{w_{xx}^{j+1}+w_{xx}^{j}}{2}\right)^{2}\mathrm{d}x\\
&\quad-\int_{-1}^{1}\frac{\rho}{2}\left(\frac{w^{1}-w^{0}}{\delta t}\right)^{2}+\frac{\gamma}{4}\left[\left(\frac{w_x^{1}+w_x^{0}}{2}\right)^{2}-1\right]^{2}+\frac{\epsilon^{2}}{2}\left(\frac{w_{xx}^{1}+w_{xx}^{0}}{2}\right)^{2}\mathrm{d}x\\
&=-\delta t\sum_{k=1}^{j}\left\{\int_{-1}^{1}\beta\left(\frac{w_x^{k+1}-w_x^{k-1}}{2\delta t}\right)^{2}\left[1+\left(w_x^{k}\right)^{2}\right]\mathrm{d}x-\int_{-1}^{1}f\left(\frac{w^{j+1}-w^{j-1}}{2\delta t}\right)\mathrm{d}x\right.\\
&\quad-\beta\frac{w^{j+1}(1)-w^{j-1}(1)}{2\delta t}\left[1+\left(w_x^{j}(1)\right)^{2}\right]+\beta\frac{w^{j+1}(-1)-w^{j-1}(-1)}{2\delta t}\left[1+\left(w_x^{j}(-1)\right)^{2}\right]\\
&\quad+\gamma\frac{w^{j+1}(1)-w^{j-1}(1)}{2\delta t}\left[\left(w_{xx}^{j}(1)\right)^{3}-w_{xx}^{j}(1)\right]-\gamma\frac{w^{j+1}(-1)-w^{j-1}(-1)}{2\delta t}\left[\left(w_{xx}^{j}(-1)\right)^{3}-w_{xx}^{j}(-1)\right]\\
&\quad+\epsilon^{2}\frac{w_x^{j+1}(1)-w_x^{j-1}(1)}{2\delta t}w_{xx}^{j}(1)-\epsilon^{2}\frac{w_x^{j+1}(-1)-w_x^{j-1}(-1)}{2\delta t}w_{xx}^{j}(-1)-\epsilon^{2}\frac{w^{j+1}(1)-w^{j-1}(1)}{2\delta t}w_{xxx}^{j}(1)\\
&\quad\left.+\epsilon^{2}\frac{w^{j+1}(-1)-w^{j-1}(-1)}{2\delta t}w_{xxx}^{j}(-1)\right\}.
\end{aligned}\tag{4.18}$$

To implement Eq. (4.16) numerically, following Condette, Melcher and Süli [57], the nonlinear terms are computed by using fixed point iterations. We shall let $w^{j+1,k+1}$ denote iterate $k+1$ for w at time step $j+1$. Then, in these iterations, we solve a linear boundary value problem to obtain $w^{j+1,k+1}$, $w_{xx}^{j+1,k+1}$ and $w_{xxxx}^{j+1,k+1}$ until $w^{j+1,k+1}-w^{j+1,k}$ converges to a specified tolerance in the $W^{2,2}$ norm. The fixed point iteration scheme is

$$\begin{aligned}
&\rho\frac{w^{j+1,k+1}}{\delta t^{2}}-\beta\frac{w_{xx}^{j+1,k+1}}{2\delta t}+\frac{\epsilon^{2}}{4}w_{xxxx}^{j+1,k+1}\\
&=\rho\frac{2w^{j}-w^{j-1}}{\delta t^{2}}-\beta\frac{w_{xx}^{j-1}}{2\delta t}-\frac{\epsilon^{2}}{4}\left(2w_{xxxx}^{j}+w_{xxxx}^{j-1}\right)+\beta\frac{w_{xx}^{j+1,k}-w_{xx}^{j-1}}{2\delta t}\left[2\left(w_x^{j}\right)^{2}+\left(w_x^{j}\right)^{4}\right]\\
&\quad+4\beta\frac{w_x^{j+1,k}-w_x^{j-1}}{2\delta t}\left[\left(w_x^{j}\right)^{3}+w_x^{j}\right]w_{xx}^{j}+\frac{\gamma^{2}}{2}\left[\left(\frac{w_x^{j+1,k}+w_x^{j}}{2}\right)^{3}-\left(\frac{w_x^{j+1,k}+w_x^{j}}{2}\right)\right]_{x}\\
&\quad+\frac{\gamma^{2}}{2}\left[\left(\frac{w_x^{j}+w_x^{j-1}}{2}\right)^{3}-\left(\frac{w_x^{j}+w_x^{j-1}}{2}\right)\right]_{x}+f\left(x,t^{j}\right).
\end{aligned}\tag{4.19}$$

In starting the fixed point iterations, the first iterates for w, w_x and w_{xx} are obtained by extrapolation from the previous two solutions, for example, $w^{j+1,1}=2w^{j}-w^{j-1}$. For this fully implicit scheme we will only use the Chebyshev integration formulation with a bordered banded matrix system. In the numerical examples, convergence of the iterative scheme was deemed to have been achieved once

$$\left\|w^{j,k+1}-w^{j,k}\right\|_{W^{2,2}}<10^{-14}.$$

Since the solution procedure for the linear systems found at each iterate is the same as for the IMEX scheme detailed in the previous subsection, that discussion is not repeated here. Similarly, the second order accurate starting values are obtained using extrapolation as shown in Eqs. (4.11)–(4.13).

4.3. Numerical convergence results for initial boundary value problems

In this section, the numerical convergence of Chebyshev methods to the smooth exact traveling wave solution of Eq. (4.1) given by Eq. (4.2) is examined. The convergence of the fully implicit scheme to the solution of Eq. (4.14), which has nonlinear dissipation term, is also demonstrated.

A numerical solution to Eq. (4.1) was computed using MATLAB for $x\in[-1,1]$ and from $t=0$ to $t=1$ using boundary conditions from the exact solution. The exact solution was also used to provide the initial conditions $\boldsymbol{w}^{0}$ and $\boldsymbol{w}_t^{0}$ and from these, the startup values for the numerical approximation scheme were obtained by extrapolation. The parameter values in the simulations were $\rho=2,\epsilon=0.1,\beta=0.001,\omega=1$ and $\kappa=1$, and a plot of the exact solution is in Fig. 11. Smaller values of ϵ and larger values of ρ were also tried. However, the numerical results showed that the spectral Chebyshev integration scheme which combines homogeneous and particular solutions performs even more poorly for more realistic

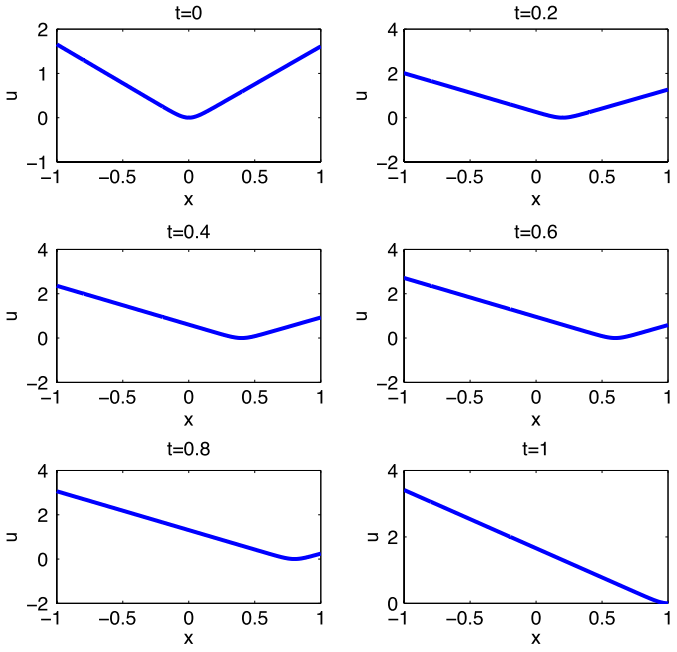

Fig. 11. Exact traveling wave solution to Eq. (4.1).

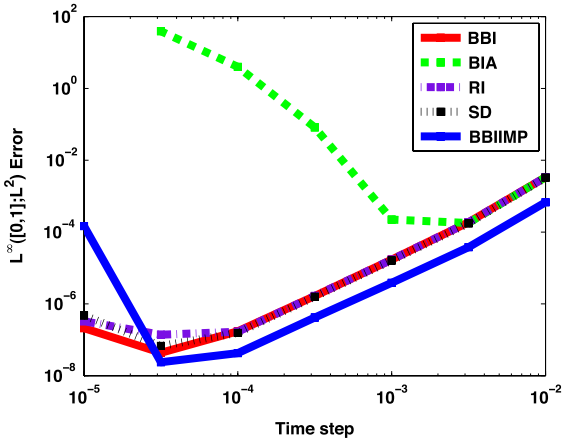

Fig. 12. $L^\infty([0,1];L^2)$ error vs. time step with 1025 Chebyshev modes. In the legend, BBI — spectral space Chebyshev integration method using the IMEX time stepping scheme where the linear systems are solved by LU factorization of the bordered banded matrix; BIA — spectral space Chebyshev integration method using the IMEX time stepping scheme where the homogeneous equation is pre-solved analytically and then the inhomogeneous equations are solved by sparse LU factorization at each time step; RI — real space Chebyshev integration method using the IMEX time stepping scheme; SD — spectral space preconditioned differentiation method using the IMEX time stepping scheme where derivatives are obtained by spectral differentiation matrices at each time step; BBIIMP — spectral space Chebyshev integration method using the fully implicit time stepping scheme and the linear systems are solved by LU factorization of the bordered banded matrix.

values of capillarity and density, while the other schemes retained their convergence properties. We have therefore chosen to present a comparison using these values, even though, in typical applications ρ will be larger and ϵ smaller.

In these simulations, the maximum difference in the L^2 and $W^{2,2}$ norms between the exact solution and the numerical solution during the time interval of simulation were calculated. Figs. 12–14 show the results for simulations done with 1025 Chebyshev modes to assess how the accuracy and computation time changed as the time step was reduced. Figs. 15–17 show the results of simulations done with a fixed time step of 10^{-3} to assess how the accuracy and computation time changed as the number of modes increased. In measuring the computational time in these simulations, only the time required for time stepping was measured, because the main interest is in estimating computation times for simulations which require many time steps and for which the setup time is a negligible proportion of the total time required.

Fig. 12 shows that the real space Chebyshev integration method and the preconditioned Chebyshev method are as accurate as the Chebyshev integration method when the full linear system is solved, but Fig. 17 shows that they are computationally more expensive. This is expected because the Chebyshev differentiation matrices in spectral space are

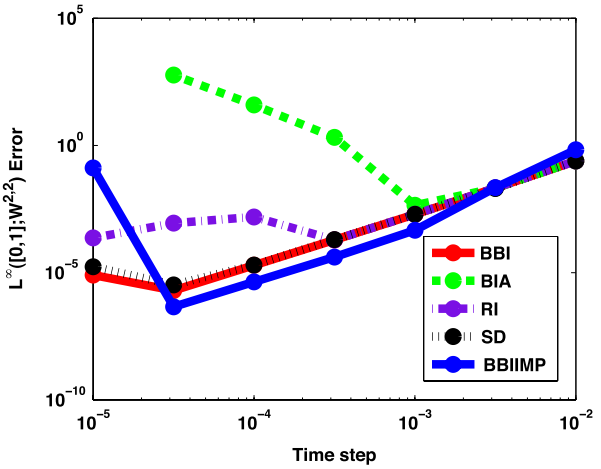

Fig. 13. $L^{\infty}([0, 1]; W^{2,2})$ error vs. time step with 1025 Chebyshev modes. In the legend, BBI — spectral space Chebyshev integration method using the IMEX time stepping scheme where the linear systems are solved by LU factorization of the bordered banded matrix; BIA — spectral space Chebyshev integration method using the IMEX time stepping scheme where the homogeneous equation is pre-solved analytically and then the inhomogeneous equations are solved by sparse LU factorization at each time step; RI — real space Chebyshev integration method using the IMEX time stepping scheme; SD — spectral space preconditioned differentiation method using the IMEX time stepping scheme where derivatives are obtained by spectral differentiation matrices at each time step; BBIIMP — spectral space Chebyshev integration method using the fully implicit time stepping scheme and the linear systems are solved by LU factorization of the bordered banded matrix.

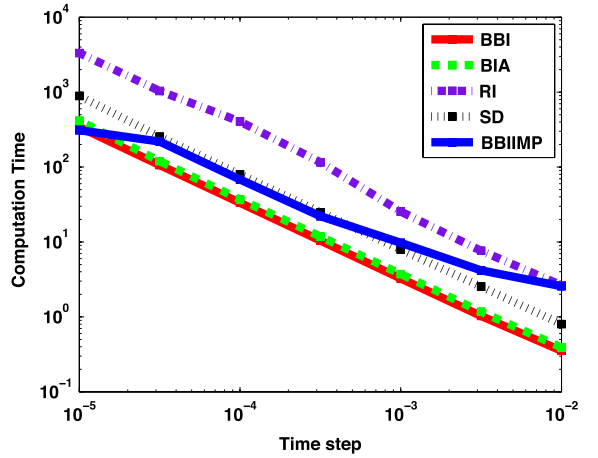

Fig. 14. Computation time vs. time step with 1025 Chebyshev modes. In the legend, BBI — spectral space Chebyshev integration method using the IMEX time stepping scheme where the linear systems are solved by LU factorization of the bordered banded matrix; BIA — spectral space Chebyshev integration method using the IMEX time stepping scheme where the homogeneous equation is pre-solved analytically and then the inhomogeneous equations are solved by sparse LU factorization at each time step; RI — real space Chebyshev integration method using the IMEX time stepping scheme; SD — spectral space preconditioned differentiation method using the IMEX time stepping scheme where derivatives are obtained by spectral differentiation matrices at each time step; BBIIMP — spectral space Chebyshev integration method using the fully implicit time stepping scheme and the linear systems are solved by LU factorization of the bordered banded matrix.

dense upper triangular matrices, the Chebyshev integration matrices in real space are dense and full, but the Chebyshev integration matrices in spectral space are sparse. Surprisingly, the actual computational cost of solving the bordered banded matrix system that immediately satisfies the boundary conditions was less than first pre-solving to obtain homogeneous solutions and then repeatedly solving banded systems for particular solutions to which linear combinations of the solutions to the homogeneous equation were added to satisfy the boundary conditions. The reason for the difference is that the computational cost of adding the homogeneous solutions to the particular solution outweighs the savings in solving a banded matrix system.

Figs. 12–14 show that for a given time step, when less than 129 discretization points are used, it is faster to use the real space Chebyshev integration method, than the spectral space Chebyshev integration method. This is not surprising since as explained in [16, p. 90], it can be computationally quicker to use the matrix multiply version of the Fourier transform instead of the Fast Fourier Transform when solving small problems. Although the fully implicit scheme is computationally more costly than the IMEX schemes, it has better L^2 accuracy. In particular, for a time step of 10^{-4}, the implicit scheme is five times more accurate in the L^2 norm than the IMEX scheme but it only takes twice as long to compute. Figs. 13 and 14

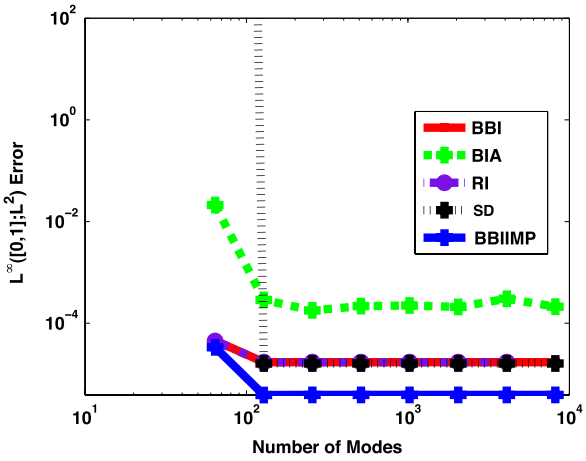

Fig. 15. $L^\infty([0,1];L^2)$ error vs. number of Chebyshev modes with a time step of 10^{-3}. In the legend, BBI — spectral space Chebyshev integration method using the IMEX time stepping scheme where the linear systems are solved by LU factorization of the bordered banded matrix; BIA — spectral space Chebyshev integration method using the IMEX time stepping scheme where the homogeneous equation is pre-solved analytically and then the inhomogeneous equations are solved by sparse LU factorization at each time step; RI — real space Chebyshev integration method using the IMEX time stepping scheme; SD – spectral space preconditioned differentiation method using the IMEX time stepping scheme where derivatives are obtained by spectral differentiation matrices at each time step; BBIIMP – Chebyshev integration method using the fully implicit time stepping scheme and the linear systems are solved by LU factorization of the bordered banded matrix.

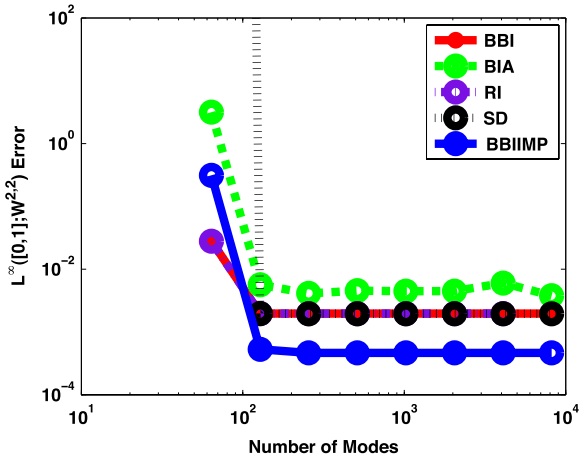

Fig. 16. $L^\infty([0,1];W^{2,2})$ error vs. number of Chebyshev modes with a time step of 10^{-3}. In the legend, BBI — spectral space Chebyshev integration method using the IMEX time stepping scheme where the linear systems are solved by LU factorization of the bordered banded matrix; BIA — spectral space Chebyshev integration method using the IMEX time stepping scheme where the homogeneous equation is pre-solved analytically and then the inhomogeneous equations are solved by sparse LU factorization at each time step; RI — real space Chebyshev integration method using the IMEX time stepping scheme; SD – spectral space preconditioned differentiation method using the IMEX time stepping scheme where derivatives are obtained by spectral differentiation matrices at each time step; BBIIMP — spectral space Chebyshev integration method using the fully implicit time stepping scheme and the linear systems are solved by LU factorization of the bordered banded matrix.

show that the conclusions in the $W^{2,2}$ norm have similar trends provided the time step is not too small or too large. One exception to this is that the $W^{2,2}$ error for the real space Chebyshev integration method begins to increase once the time step is less than 0.5×10^{-3} due to finite precision effects. These are made worse by the large number of operations required for dense matrices.

Again, examining Figs. 12 and 13 we find that combining solutions of the homogeneous boundary value problem with the solution of the inhomogeneous boundary value problem solved at each time step gives poor accuracy when the time step is less than 10^{-3}. The reason for the poor accuracy in the time dependent case is that rounding errors obtained when satisfying the boundary conditions accumulate at each time step — we note that the initial curve has a second order convergence rate, and then displays the characteristic 'U' shape that is typically observed when rounding errors dominate. The reason for the poor accuracy is not that the diagonal banded portion of the matrix system is not strictly diagonally dominant — it is known that linear systems that are strictly diagonally dominant can be solved in a numerically stable manner (see, for example, Higham [46, p. 170]), for linear systems that are not strictly diagonally dominant, it is in general difficult to prove that the resulting system can be solved in a numerically stable manner. This is because all three implementations of the Chebyshev

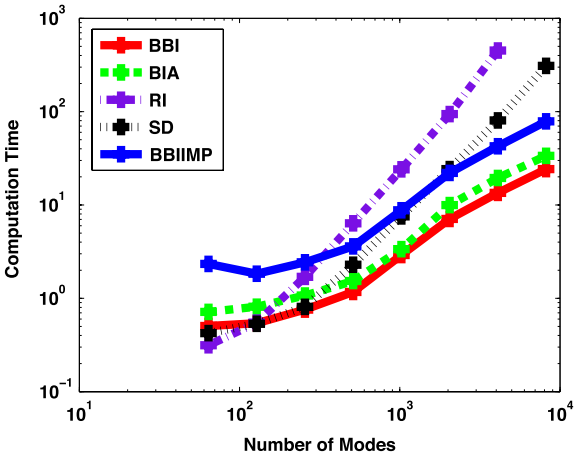

Fig. 17. Computation time vs. number of Chebyshev modes with a time step of 10^{-3}. In the legend, BBI — spectral space Chebyshev integration method using the IMEX time stepping scheme where the linear systems are solved by LU factorization of the bordered banded matrix; BIA — spectral space Chebyshev integration method using the IMEX time stepping scheme where the homogeneous equation is pre-solved analytically and then the inhomogeneous equations are solved by sparse LU factorization at each time step; RI — real space Chebyshev integration method using the IMEX time stepping scheme; SD — spectral space preconditioned differentiation method using the IMEX time stepping scheme where derivatives are obtained by spectral differentiation matrices at each time step; BBIIMP — Chebyshev integration method using the fully implicit time stepping scheme and the linear systems are solved by LU factorization of the bordered banded matrix.

integration method discussed here were equally accurate for the linear boundary value problem Eq. (3.38), which has a similar structure to the boundary value problem solved at each time step when the time step is small. We conclude that for boundary value problems, there is no time integration, so the effect of rounding errors created by enforcing the boundary conditions does not grow. Higham [46, p. 79] explains that it is possible to use compensated summation to reduce the cumulative effect of rounding errors when obtaining multiplicative coefficients for the homogeneous solutions and adding them to the particular solution. We have not investigated the effectiveness of compensated summation because it depends on how floating point operations are implemented, and so it is not a portable method for reducing the effects of rounding errors.

Figs. 15–17 show how the computational accuracy and computational time vary as the number of modes is increased. Again, it is fastest to use the spectra space Chebyshev integration method and solve the bordered banded matrix system rather than to obtain a particular solution to which solutions of the homogeneous boundary value problem are added. When more than 257 Chebyshev modes are used, it is more computationally costly to use the spectral space preconditioned differentiation Chebyshev method with spectral differentiation in the IMEX time stepping schemes.

A particularly interesting feature in Figs. 15 and 16 is that, as the number of modes is increased, a smaller time step is not required to ensure the stability of the IMEX schemes. Greengard [25] has hinted that the spectral space Chebyshev integration method may overcome the time step restrictions for explicit time stepping schemes using the real space Chebyshev differentiation method pointed out in [20,21]. Trefethen and Embree [58, p. 287] review the stability of spectral spatial discretizations of initial boundary value problems and show that due to small perturbations introduced by finite precision arithmetic, the solutions to linear systems obtained during time stepping with real space Chebyshev differentiation matrices are poor approximations of the actual solutions. Trefethen and Embree [58] show that only very small perturbations are needed to make large Chebyshev differentiation matrices singular. The Chebyshev spectral integration matrices used here are not normal, but their eigenvalues and singular values are clustered near the origin in such a manner that, as the size of the discretization grows, the largest eigenvalues and singular values are bounded independently of the size of the discretization. This would suggest that, provided the resulting linear systems are solved accurately, IMEX time stepping methods using Chebyshev integration matrices will have stability properties that are independent of the spatial resolution.

Finally, Fig. 18 shows the exact solution to Eq. (4.14) given by Eq. (4.15) plotted over the simulation time. Fig. 19 demonstrates second order convergence of the implicit scheme in Eq. (4.16) and Fig. 20 demonstrates that energy is approximately conserved by the numerical method. In these simulations 1025 Chebyshev modes were used and the physical parameters were $\rho = 1.0, \epsilon = 10^{-1}$ and $\beta = 1.0$.

5. Discussion

We have used fixed time stepping schemes in comparing the different collocation Chebyshev methods. The equations for viscoelastic dynamics with small capillarity can exhibit long lived metastable states. For such equations, significant reductions in computation times can be obtained by using adaptive time stepping.

We have only examined collocation and pseudospectral methods. These have errors due to aliasing because in collocation, the residual at the discretization points is made to be zero — this introduces unresolved high frequencies which implies that the solution obtained is not quite as good as the best approximation in the natural Chebyshev norm even though it

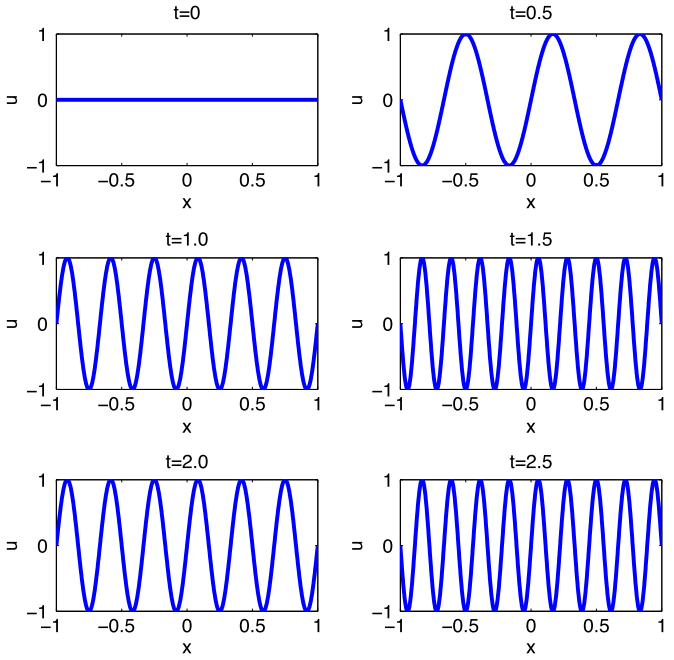

Fig. 18. Exact solution to Eq. (4.14) given by Eq. (4.15).

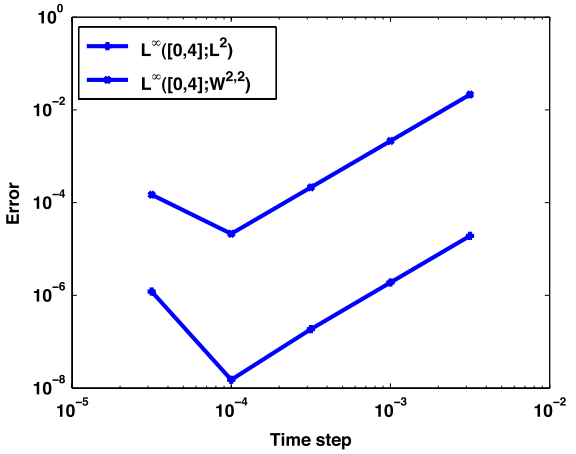

Fig. 19. Temporal convergence results for the fully implicit scheme Eq. (4.16) for the numerical solution of the initial boundary value problem with nonlinear dissipation given in Eq. (4.14) with 1025 Chebyshev modes.

has the same order of accuracy. Similarly when nonlinear terms are computed by pseudospectral methods, unresolved high frequencies are introduced which imply that the approximation is not quite as good as the best approximation in the natural Chebyshev norm. To get the best approximation in the Chebyshev norm, Galerkin methods should be used. However, our results indicate that since the Chebyshev integration formulation in spectral space is sparse, for a wide range of problems, it is computationally feasible to obtain accuracy that is correct to machine precision. Shen [59] has shown that sparse Chebyshev Galerkin approximations can be constructed using some of the relationships between Chebyshev polynomials that were used in the construction of the Chebyshev integration method. Unfortunately, Shen's [59] algorithm scales like $O(N^2)$ for one dimensional fourth order problems and is ill-conditioned, so cannot be used for high resolution simulations. It seems likely that a Galerkin implementation of the Chebyshev integration method similar to that used in [33] would be well conditioned and would also scale like $O(N \log N)$, provided that any nonlinear terms could be solved using a scalable iterative procedure, such as the fixed point implementation in Eq. (4.19). We leave the exploration of this idea for future work.

6. Conclusion

The spectral space Chebyshev integration method allows one to obtain high resolution simulations to semilinear initial boundary value problems on finite non-periodic intervals with time dependent boundary conditions. If less than 100 modes

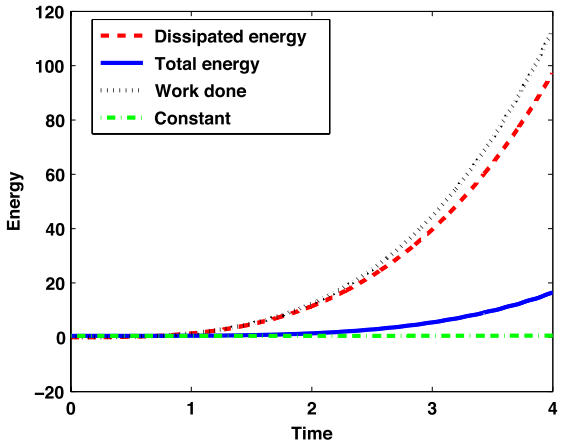

Fig. 20. Demonstration that the variational scheme exhibits conservation of energy when approximating Eq. (4.14) using a time step of $10^{-4.5}$ and 1025 Chebyshev modes. The dissipation is given by $\int_0^T \int_{-1}^1 \beta w_{xt}^2(1+w_x^2)\mathrm{d}x\mathrm{d}t$, the total energy by $\int_{-1}^1 \frac{\rho}{2} w_t^2 + \frac{\gamma}{4}\left(w_x^2-1\right)^2 + \frac{\epsilon^2}{2} w_{xx}^2 \mathrm{d}x$ and the work done by $\int_0^T \int_{-1}^1 f w_t \mathrm{d}x\mathrm{d}t$. To check whether conservation of energy holds, we check that Total Energy + Dissipated energy − Work done = Constant.

are required and accurate results in the L^2 norm are needed, the standard real space Chebyshev differentiation method is easiest to use. If less than 100 modes are required and accurate results in the $W^{2,2}$ norm are needed, the real space Chebyshev integration method is most appropriate. If high resolution simulations are required, and the function only needs to be approximated correctly in the L^2 norm, then the preconditioned Chebyshev differentiation method is the best method to apply. When a wide range of scales are present in smooth solutions to high order initial boundary value problems and spatial derivatives of the function need to be estimated, then the spectral space Chebyshev integration method is the most appropriate method to be used for numerical investigation of these solutions.

Acknowledgements

The author is most grateful to Nick Trefethen for making many helpful suggestions. He also thanks Endre Süli, Petr Plecháč and John Ball for their encouragement and advice during this work. The work on variational integrators was greatly influenced by a very helpful set of discussions with Melvin Leok. The author also thanks Lindy Castell, Nicolas Condette, Toby Driscoll, Richard Norton, Christoph Ortner, Tomas Roubicek, Umut Salman and Wynn Tee for their constructive criticism and numerous suggestions. Finally he acknowledges very helpful comments made by two anonymous readers. In particular, one of the readers is thanked for suggesting examination of the accuracy of solutions obtained using the preconditioned Chebyshev differentiation method with derivatives obtained using spectral differentiation matrices. The support of the MULTIMAT Marie Curie Research Training Network (MRTN-CT-2004-505226) is gratefully acknowledged.

References

[1] R. Ahluwalia, T. Lookman, A. Saxena, Dynamic strain loading of cubic to tetragonal martensites, Acta Mater. 54 (2006) 2109–2120.
[2] K.-H. Hoffmann, P. Rybka, On convergence of solutions to the equation of viscoelasticity with capillarity, Comm. Partial Differential Equations 25 (2000) 1845–1890.
[3] L. Truskinovsky, Kinks versus shocks, in: J.E. Dunn, R. Fosdick, M. Slemrod (Eds.), Shock induced transitions and phase structures in general media, in: IMA Vol. Math. Appl., volume 52, 1993, pp. 185–229.
[4] A. Vainchtein, Stick-slip interface motion as a singular limit of the viscosity-capillarity model, Math. Mech. Solids 6 (3) (2001) 323–341.
[5] P. Dondl, J. Zimmer, Modeling and simulation of martensitic phase transitions with a triple point, J. Mech. Phys. Solids 52 (2004) 2057–2077.
[6] M. Luskin, On the computation of crystalline microstructure, Acta Numer. 5 (1996) 191–258.
[7] C. Xu, T. Tang, Stability analysis of large time-stepping methods for epitaxial growth models, SIAM J. Numer. Anal. 44 (2006) 1759–1779.
[8] A.-K. Kassam, L.N. Trefethen, Fourth-order time stepping for stiff pdes, SIAM J. Sci. Comput. 26 (4) (2005) 1214–1233.
[9] G.-Q. Chen, Q. Du, E. Tadmor, Spectral viscosity approximations to multidimensional scalar conservation laws, Math. Comp. 61 (204) (1993) 629–643.
[10] J.S. Hesthaven, S. Gottlieb, D. Gottlieb, Spectral Methods for Time-dependent Problems, Cambridge University Press, 2007.
[11] Y. Kaneda, T. Ishihara, High resolution direct numerical simulation of turbulence, J. Turbulence 7 (20) (2006) 1–17.
[12] P. Yeung, Lagrangian investigations of turbulence, Annu. Rev. Fluid Mech. 34 (2002) 115–142.
[13] J. Jiménez, R. Moser, What are we learning from simulating wall turbulence?, Philos. Trans. Roy. Soc. A. 365 (2007) 715–732.
[14] D. Torres, E.A. Coutsias, Pseudospectral solution of the two-dimensional Navier–Stokes equations in a disk, SIAM J. Sci. Comput. 21 (1) (1999) 378–403.
[15] D. Gottlieb, S.A. Orszag, Numerical Analysis of Spectral Methods: Theory and Applications, SIAM, 1977.
[16] C. Canuto, M.Y. Hussaini, A. Quarteroni, T. Zang, Spectral Methods Fundamental in Single Domains, Springer, 2006.
[17] E.A. Coutsias, T. Hagstrom, D. Torres, An efficient spectral method for ordinary differential equations with rational function coefficients, Math. Comp. 65 (214) (1996) 611–635.
[18] D. Funaro, W. Heinrichs, Some results about the pseudospectral approximation of one-dimensional fourth-order problems, Numer. Math. 58 (1990) 399–418.
[19] L.S. Tuckerman, Transformations of matrices into banded form, J. Comput. Phys 84 (1989) 360–376.
[20] L.N. Trefethen, M.R. Trummer, An instability phenomenon in spectral methods, SIAM J. Numer. Anal. 24 (5) (1987) 1008–1023.
[21] J.A.C. Weideman, L.N. Trefethen, The eigenvalues of second-order spectral differentiation matrices, SIAM J. Numer. Anal. 25 (6) (1988) 1279–1298.

[22] C.W. Clenshaw, The numerical solution of linear differential equations in Chebyshev series, Proc. Cambridge Phil. Soc. 53 (1957) 134–149.
[23] S.E. El-Gendi, Numerical treatment of differential equations and integral equations, Ph.D. thesis, University of Southampton, 1964.
[24] S.E. El-Gendi, Chebyshev solution of differential integral and integro-differential equations, Comput. J. 12 (1969) 282–287.
[25] L. Greengard, Spectral integration and two-point boundary value problems, SIAM J. Numer. Anal. 28 (4) (1991) 1071–1080.
[26] M. Hiegemann, Chebyshev matrix operator method for the solution of integrated forms of linear ordinary differential equations, Acta Mech. 122 (1997) 231–242.
[27] A.K. Khalifa, E.M.E. Elbarbary, M.A. Abd Elrazek, Chebyshev expansion method for solving second and fourth-order elliptic equations, Appl. Math. Comput. 135 (2003) 307–318.
[28] S.M. Cox, P.C. Matthews, A pseudospectral code for convection with an analytical/numerical implementation of horizontal boundary conditions, Int. J. Numer. Meth. Fluids 25 (1997) 151–166.
[29] A. Lundbladh, D.S. Hennigson, A.V. Johansson, An efficient spectral integration method for the solution of the Navier–Stokes equations, Technical Report FFA-TN 1992-28, Aeronautical Research Institute of Sweden, 1992.
[30] D. Elliot, A method for the numerical integration of the one-dimensional heat equation using Chebyshev series, Proc. Cambridge Phil. Soc. 57 (1960) 823–832.
[31] A.H. Khater, R.S. Temsah, Numerical solutions of some nonlinear evolution equations by Chebyshev spectral collocation methods, Int. J. Comput. Math. 84((3) (2007) 305–316.
[32] A.H. Khater, R.S. Temsah, Numerical solutions of the generalized Kuramoto-Sivashinsky equation by Chebyshev spectral collocation methods, Comput. Math. Appl. 56 (2008) 1465–1472.
[33] A. Zebib, A Chebyshev method for the solution of boundary value problems, J. Comput. Phys. 53 (1984) 443–455.
[34] N. Mai-Duy, An effective spectral collocation method for the direct solution of high-order odes, Commun. Numer. Meth. Engng. 22 (2006) 627–642.
[35] N. Mai-Duy, R. Tanner, A spectral collocation method based on integrarted Chebyshev polynomials for two-dimensional biharmonic boundary-value problems, J. Comput. and Appl. Math. 201 (2007) 30–47.
[36] K.T. Elgindy, Generation of higher order pseudospectral integration matrices, Appl. Math. Comput. 209 (2009) 153–161.
[37] T.A. Driscoll, Automatic spectral collocation for integral equations. Pre-print, 2009.
[38] A. Deloff, Semi-spectral Chebyshev method in quantum mechanics, Ann. Phys. 322 (2007) 1373–1419.
[39] B. Mihalia, I. Mihalia, Numerical approximations using Chebyshev polynomial expansions: El-Gendi's method revisited, J. Phys. A: Math. Gen. 35 (2002) 731–746.
[40] M.S. Stern, Application of the El-Gendi method to the Schrödinger integral equation, J. Comput. Phys. 28 (1978) 122–128.
[41] L.N. Trefethen, Spectral Methods in MATLAB, SIAM, 2000.
[42] A.T. Patera, A spectral element method for fluid dynamics: Laminar flow in a channel expansion, J. Comput. Phys. 54 (1984) 468–488.
[43] L.N. Trefethen, Is Gauss quadrature better than Clenshaw-Curtis?, SIAM Rev. 50 (1) (2008) 67–87.
[44] R. Peyret, Spectral Methods for Incompressible Viscous Flow, in: Applied Mathematical Sciences, volume 148, Springer, 2002.
[45] T.A. Driscoll, Cumsummat. A MATLAB program to compute the real space Chebyshev integration matrix, May 2008.
[46] N. Higham, Accuracy and Stability of Numerical Algorithms, SIAM, 2006.
[47] L. Truskinovskii, Equilibrium phase interfaces, Sov. Phys. Dokl. 27 (7) (1982) 551–552.
[48] T. Davis, Suitesparse, www.cise.ufl.edu/research/sparse/.
[49] T. Davis, Direct Methods for Sparse Linear Systems, SIAM, 2006.
[50] W. Kress, Error estimates for deferred correction methods in time, Appl. Numer. Math. 57 (2007) 335–353.
[51] E. Hairer, C. Lubich, G. Wanner, Geometric Numerical Integration, second edition, in: Springer Series in Computational Mathematics, Springer, 2006.
[52] C. Kane, J.E. Marsden, M. Ortiz, M. West, Variational integrators and the Newmark algorithm for conservative and dissipative mechanical systems, Int. J. Numer. Meth. Engng. 49 (2000) 1295–1325.
[53] M. Leok, Foundations of computational geometric mechanics, Ph.D. thesis, Caltech, 2004.
[54] A. Lew, Variational time integrators in computational solid mechanics, Ph.D. thesis, Caltech, 2003.
[55] A. Lew, J.E. Marsden, M. Ortiz, M. West, Variational time integrators, Int. J. Numer. Meth. Engng. 60 (2004) 153–212.
[56] J.E. Marsden, M. West, Discrete mechanics and variational integrators, Acta Numer. 10 (2001) 357–514.
[57] N. Condette, C Melcher, E. Süli, Spectral approximations of pattern-forming nonlinear evolution equations with double-well potentials of quadratic growth. Math. Comput. (in press). A pre-print version can be found at http://web.comlab.ox.ac.uk/people/Endre.Suli/biblio.html.
[58] L.N. Trefethen, M. Embree, Spectra and Pseudospectra, Princeton, 2005.
[59] J. Shen, Efficient spectral-Galerkin method II. Direct solvers of second and fourth order equations by using Chebyshev polynomials, SIAM J. Sci. Comput. 16 (2) (1995) 74–87.